A Digital Spectral Classification Atlas

R. O. Gray

Dept. of Physics and Astronomy

Appalachian State University

v. 1.07

January 30, 2009

Introduction

The MK Spectral classification system was founded by W.W. Morgan and P.C. Keenan in the year 1943, with the publication of the first photographic spectral classification atlas, *An Atlas of Stellar Spectra* (Morgan, Keenan & Kelleman, 1943). Since that time, the MK system has been extensively revised and refined by Morgan, Keenan and others. In the late 1970's, two important spectral atlases, summarizing the development of the MK system up to that time, were published. These atlases, the *Revised MK Spectral Atlas for Stars Earlier than the Sun* by Morgan, Abt & Tapscott (1978) and *An Atlas of Spectra of the Cooler Stars: Types G,K,M,S and C*, by Keenan & McNeil (1976), are the inspiration for the various versions of this digital spectral classification atlas. Indeed, some of the pages in this atlas are "digitized" versions of pages from those two atlases.

The MK spectral classification system is a natural, empirical system of classification which uses in the classification process only the directly observable features in the spectrum. The MK system is defined by a set of standard stars, and classification on the system is carried out by the comparison of the program star with the standard stars, taking into account all of the features in the spectrum. The use of standards is vital because it maintains the autonomy of the system as well as ensuring that different observers will classify stars on the same system.

When the MK system was first defined, it was based on photographic spectra in the blue-violet part of the spectrum. This was done by necessity, as scientific photographic emulsions in the 1940's were sensitive only to blue-violet light. However, it was a fortunate choice, as the blue-violet portion of the spectrum (essentially from the Ca II K-line to Hβ) contains a high density of astrophysically important atomic lines and molecular bands, which allow accurate classification of the star in a two-dimensional temperature, luminosity grid. Classification systems can and have been set up in the red, IR and the ultraviolet. These should remain independent of the traditional MK system, as different parts of the spectrum can sample different levels in the atmosphere of the star.

This version of the Digital Spectral Classification Atlas should really be considered a synopsis of the much more extensive *Stellar Spectral Classification* by R.O. Gray and C.J. Corbally, to be published by Princeton University Press in spring, 2009. Since I have borrowed extensively from that book for this atlas (all the figures in this atlas except for Figure 29 are from that book), this atlas should not be redistributed either electronically or in hardcopy form. I urge you to buy the book when it comes out!

Many, but not all of the spectra in this atlas were obtained with the Gray/Miller spectrograph on the 0.8 meter telescope of the Dark Sky Observatory (DSO), using a CCD detector. For the DSO spectra, two spectral resolutions are used in this atlas. Most of the illustrations use spectra obtained with the 1200g/mm grating, which gives a spectral resolution of 1.8Å/2 pixels and a spectral range of 3800Å – 4600Å, but some illustrations, especially those of the later-type stars (K, M, C and S) use spectra obtained with the 600g/mm grating. These have a resolution of 3.6Å/2 pixels, and a spectral range of 3800Å – 5600Å. The higher resolution spectra are presented in a rectified intensity versus wavelength format, in which the spectral continuum has been normalized to unity. The 3.6Å resolution spectra, for the most part, are presented in a flux versus wavelength format; this format provides additional information on

the energy distribution of the star, and is to be preferred for the cooler stars, as these stars have essentially no continuum points in their spectra. For ease of illustration, the fluxes have been normalized to unity at one consistent point in the spectrum.

Since the publication of the two most recent photographic spectral atlases mentioned in the paragraphs above, the MK system has undergone considerable refinement and extension. Important work in refining and extending the MK system to dimensions beyond the traditional two-dimensional temperature/luminosity grid has been carried out by Keenan and co-workers in the addition of abundance indices for the late-type stars, by Gray (1989), in the extension of the MK system to metal-weak F and G-type stars, by Kirkpatrick & coworkers in their careful redefinition and extension of the MK system to the M-type dwarfs and most lately the L- and T-type dwarfs , and by Walborn in the classification of the O-type stars. All of those developments are discussed in detail in *Stellar Spectral Classification*. Unlike earlier versions of this atlas, this atlas does not illustrate spectra of white dwarfs, novae or supernovae. If you want to explore the spectra of such stars, buy the book!
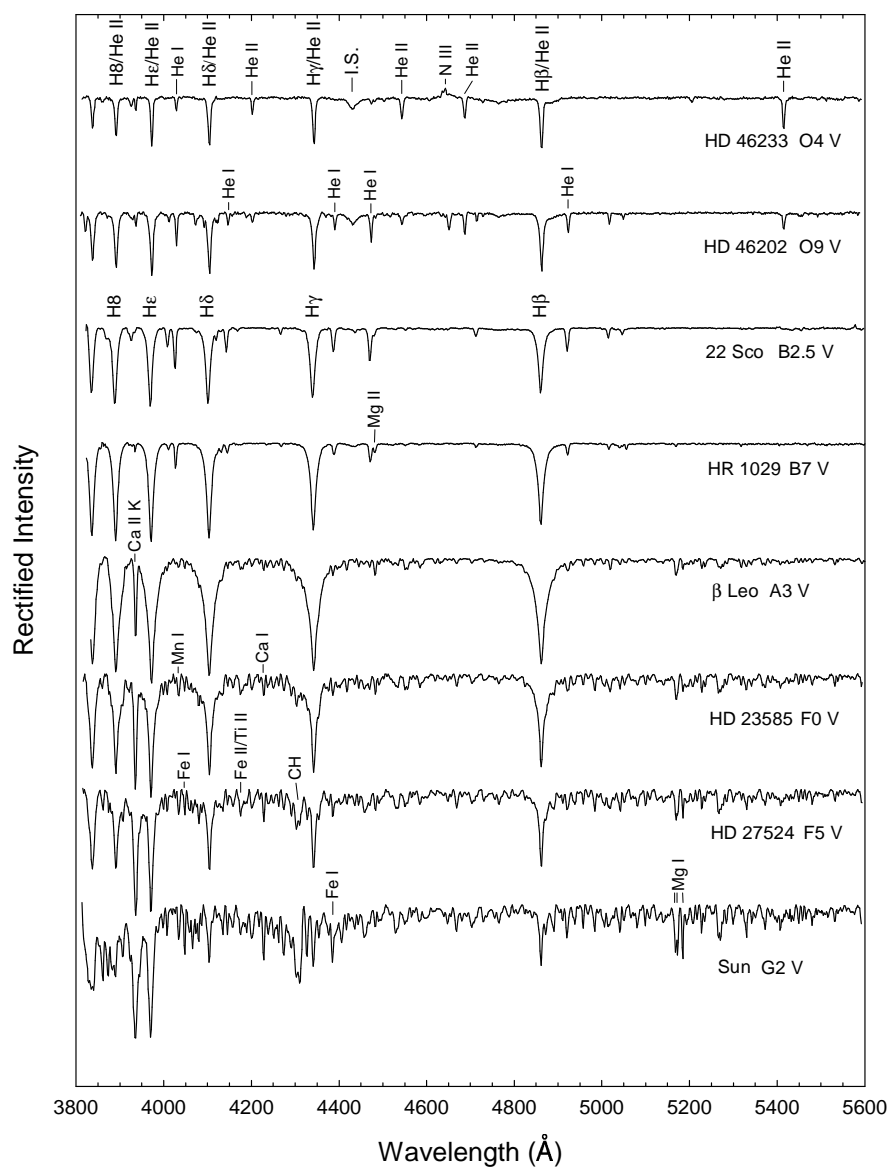
The Spectral Sequence

Figure 1: The Main Sequence from O4 to G2, the "early-type" stars.

Figures 1 and 2 show a bird's eyeview of the spectral sequence, which is dissected and examined in more detail in later portions of this atlas. Figure 1 shows the spectral sequence from the hottest "normal" stars, the O-type stars, to spectral type G2, the spectral type of our sun. The spectra of these "early-type" stars are dominated by the Balmer lines of hydrogen. Note how they increase in strength and reach a maximum at A2, and then fade

thereafter. The O- and B-type stars are characterized by lines of helium; the A-, F-, and G-type stars are characterized by lines of metals.
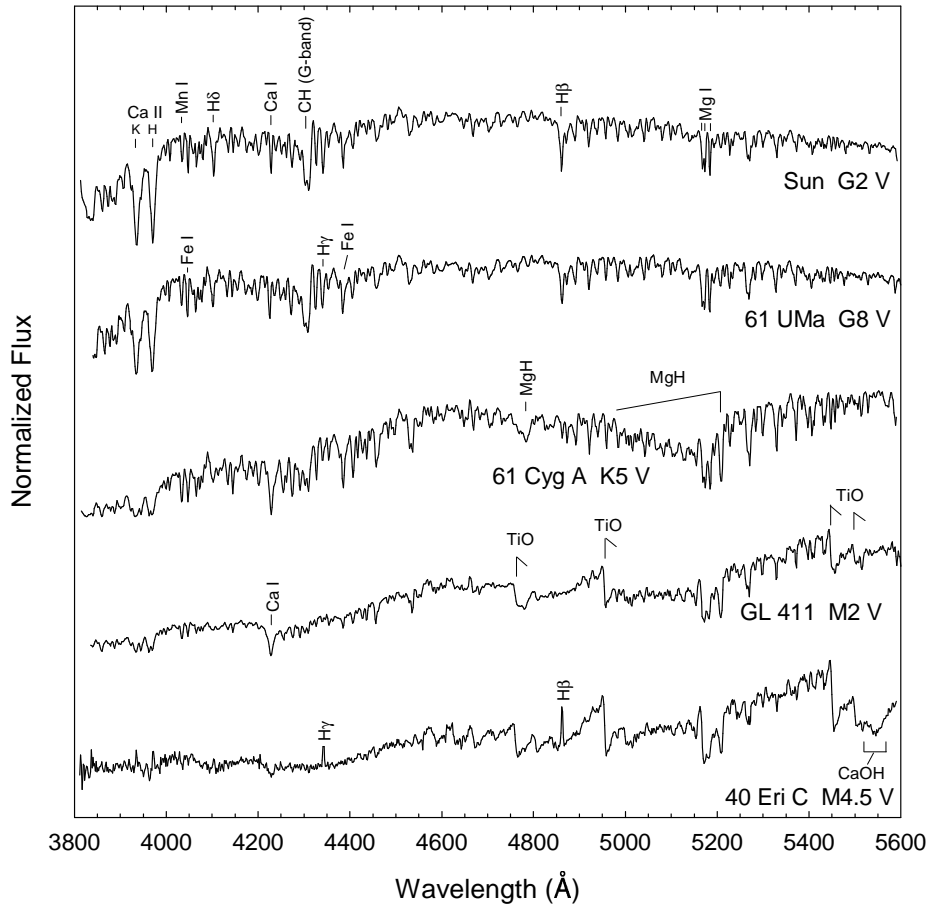

Figure 2: The Main Sequence from G2 to M4.5, the "late-type" stars.

Molecular features first appear in the spectra of F-type main sequence stars and grow to dominate the spectra of the "late-type" stars, especially those of types K and M. The main sequence does not end at M4.5, but continues through the late M-, the L- and the T-type dwarfs, a sequence that spans the transition from hydrogen-burning dwarf stars to brown dwarfs.
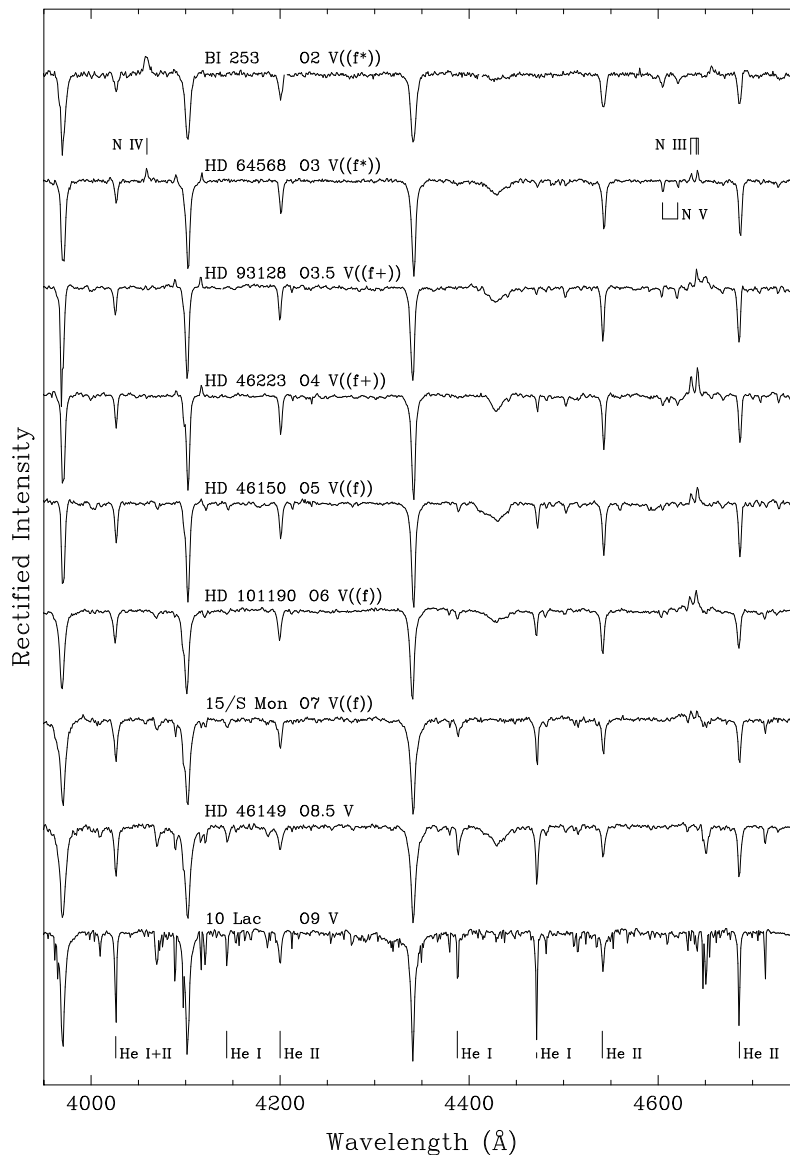
The Main Sequence O2 – O9

Figure 3: The O-type main sequence stars. Reproduced from *Stellar Spectral Classification*; original figure courtesy Ian Howarth.

The O-type stars constitute the hottest normal stars, and are characterized by moderately weak hydrogen lines, lines of neutral helium (He I) and by lines of singly ionized helium (He II). The spectral type can be judged easily by the ratio of the strengths of lines of He I to He II; He I tends to increase in strength with decreasing temperature while He II decreases in strength. The ratio He I 4471 to He II 4542 shows this trend clearly.

Visible in a number of stars in this figure is a broad, shallow depression, centered near

4430Å. This is an example of a diffuse interstellar band, probably due to molecules in the interstellar medium between us and the star.
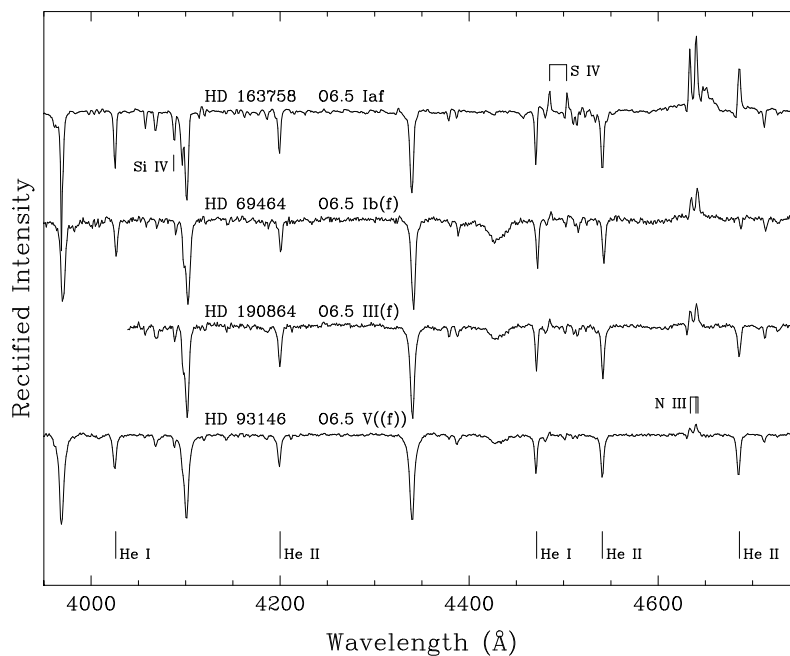
Luminosity Effects at O6.5

Figure 4: A luminosity sequence at O6.5. Figure reproduced from *Stellar Spectral Classification*; original figure courtesy I. Howarth.

Figure 4 shows a luminosity sequence at a spectral type of O6.5. At this spectral type a number of luminosity criteria are active. Note that in the O6.5 dwarf (V), the N III triplet ($\lambda\lambda4634$, 4640, 4642) is weakly in emission, but at higher luminosities the emission strength increases. The Si IV $\lambda4089$ line shows a positive luminosity effect and the hydrogen lines ($\lambda\lambda4101$, 4340) a very weak negative luminosity effect. The two S IV lines ($\lambda\lambda4486$, 4504) go into emission in the Iaf supergiant.
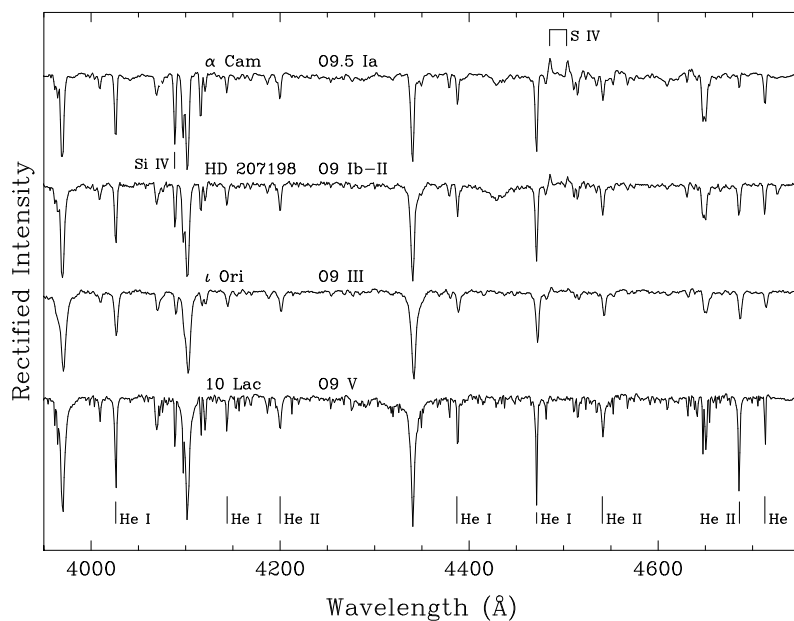
Luminosity Effects at O9

Figure 5: A luminosity sequence at O9. Figure reproduced from *Stellar Spectral Classification*; original figure courtesy I. Howarth.

At O9 the hydrogen lines show a more pronounced sensitivity to luminosity than at earlier (hotter) types. However, the primary luminosity criteria at this spectral type are the ratio of Si IV 4089 to Hδ (which becomes narrower and weaker in the more luminous stars), and the ratio of Si IV 4116 to the neighboring He I 4121 line. Note as well that the S IV lines ($\lambda\lambda$4486, 4504) go into emission in the supergiants.
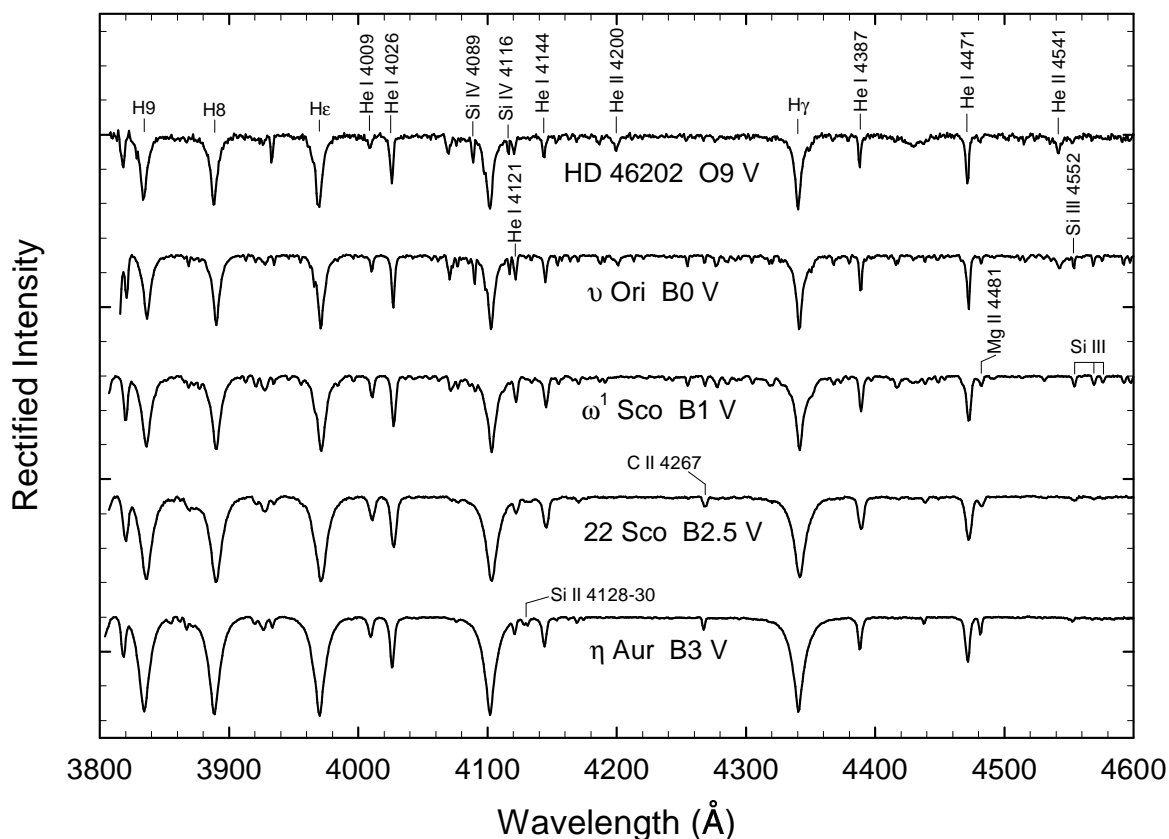
The Main Sequence O9 – B3

Figure 6: A temperature sequence in the early B-type stars.

The definition of the break between the O-type stars and the B-type stars is the absence of lines of ionized helium (He II) in the spectra of B-type stars. The lines of He I pass through a maximum at approximately B2, and then decrease in strength towards later (cooler) types. A useful ratio to judge the spectral type is the ratio He I 4471/Mg II 4481.

Were it not for the presence of helium peculiarities in both the early and late B-type stars, the behavior of He I would be sufficient to accurately estimate the spectral type in the B-type stars. However, because of these peculiarities, the spectral type in the early B-type stars is, instead, estimated on the basis of ratios of lines of silicon ions. For instance, between B0 and B1 (an interval which can be divided into B0, B0.2, B0.5, B0.7 and B1 classes), the Si IV $\lambda4089$/Si III $\lambda4552$ ratio may be used. Between B1 and B3 the Si III $\lambda4552$/Si II $\lambda4128$-32 ratio may be used.
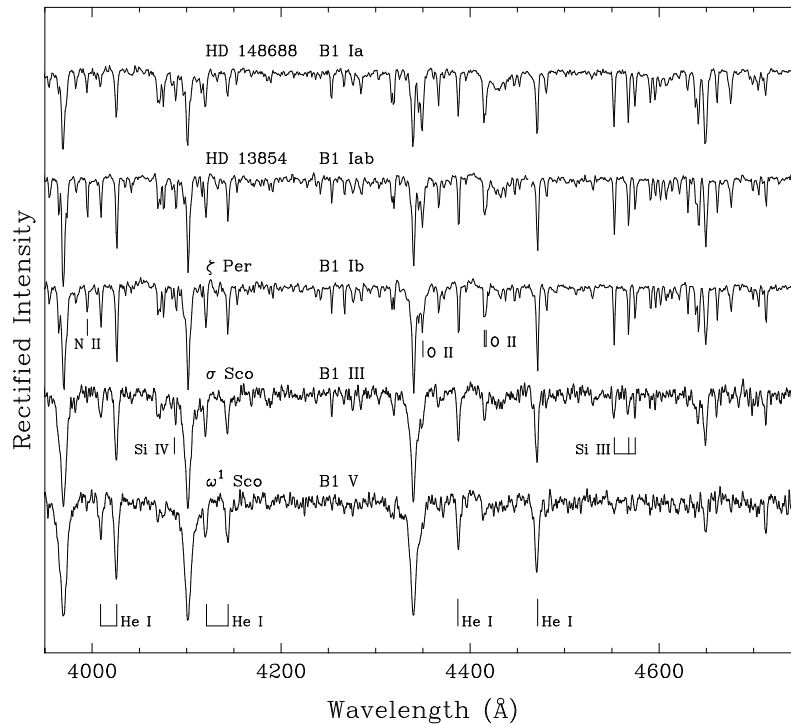
Luminosity Effects at B1

Figure 7: A luminosity sequence at B1. Figure reproduced from *Stellar Spectral Classification*; original figure courtesy I. Howarth.

While the width and strength of the hydrogen lines is a useful luminosity criterion at B1, the sensitivity of the O II lines (see O II 4070, 4348 and 4416), especially in ratio with adjacent hydrogen lines and the He I lines (which tend to weaken with increasing luminosity) helps to increase the precision of luminosity classification at B1. However, the discovery of oxygen and carbon peculiarities in the early B-type stars means that those ratios should be used with caution. As a consequence, the luminosity classification in the early B-type stars (B2 and earlier) has shifted to ratios of lines of ionized silicon to neutral helium. In particular, the Si IV λ4116/He I λ4121 ratio is useful earlier than B0.7, whereas the Si III λ4552/He I λ4387 is useful later than B0.7.
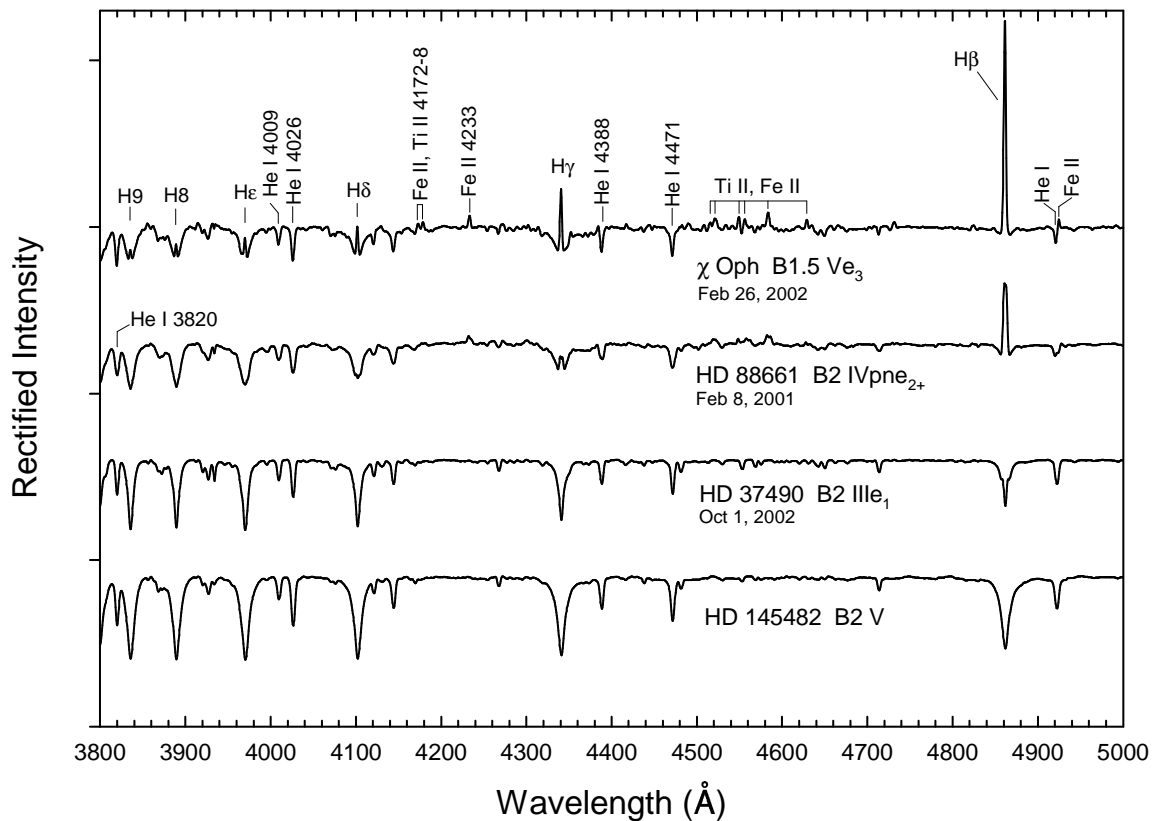
The Be Stars

Figure 8: A selection of Be stars compared with a B2 V secondary standard, HD 145482. The spectral types are on the Lesh (1968) system. Spectra from the Paranal Observatory spectral library.

The Be stars are B-type stars that are characterized (or have been characterized in the past) by emission in one or more of the Balmer lines of hydrogen, sometimes accompanied by emission in lines of singly ionized metals, most commonly Fe II. The Be class excludes B-type supergiants, as well as pre main-sequence stars such as the Herbig Ae/Be stars. Many Be stars may be classified without difficulty on the MK system, although the more extreme present significant difficulties. Lesh (1968) introduced an extension to the MK system for the Be stars comprised of an "e" index (e1 $\rightarrow$ e4, in direction of increasing emission-line strength). Some typical Be spectra are illustrated in Figure 8.
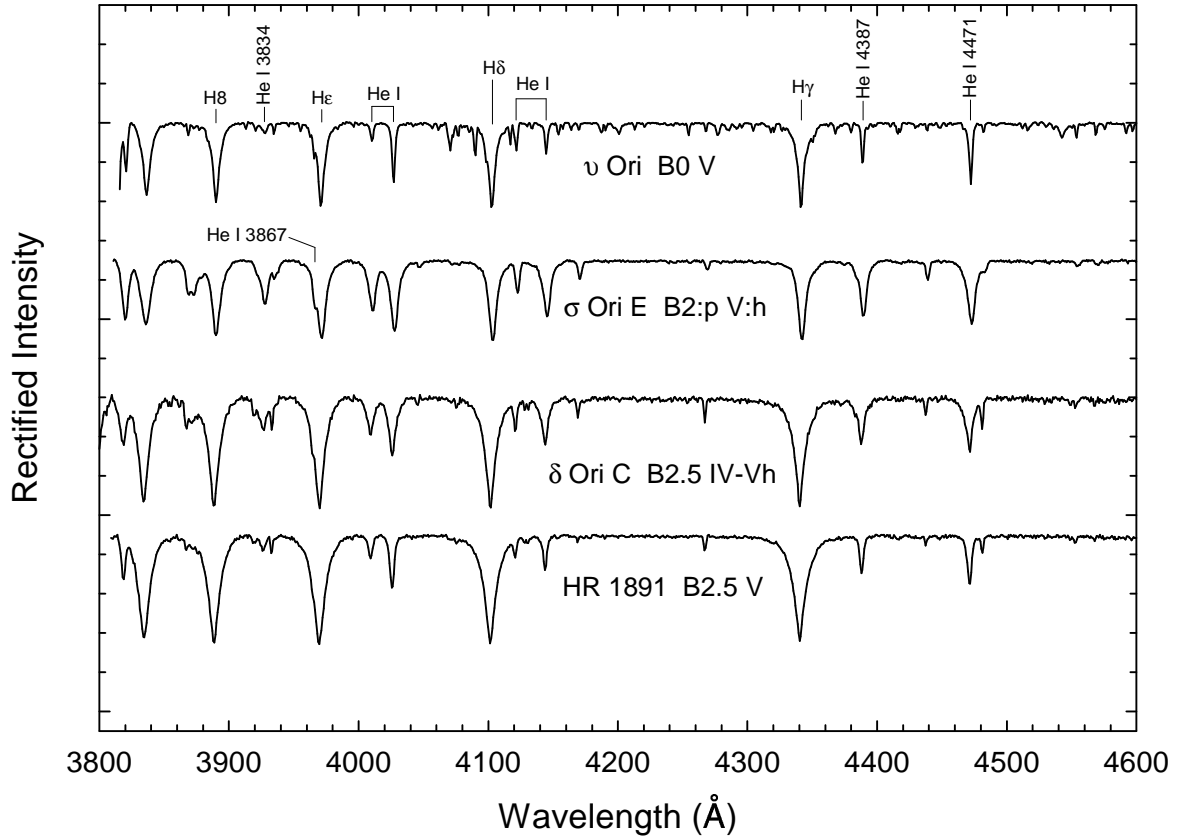
Helium-Strong B-type Stars

Figure 9: Two helium-strong stars, σ Ori E and δ Ori C compared with two MK standards. Dark Sky Observatory (DSO) 1.8Å resolution spectra.

Some early B-type stars (earlier than B3) show extraordinarily strong lines of He I. Two examples, illustrated above, are σ Ori E and δ Ori C. Some of these stars are spectroscopic variables in that the He I lines vary in strength with the rotational period of the star. Many of these stars have strong magnetic fields; it is believed that the helium concentrates at one or both of the magnetic poles. As the pole rotates in and out of sight, the He I line strengths vary. To indicate a star's helium-strong status, an "h" is appended to the spectral type.
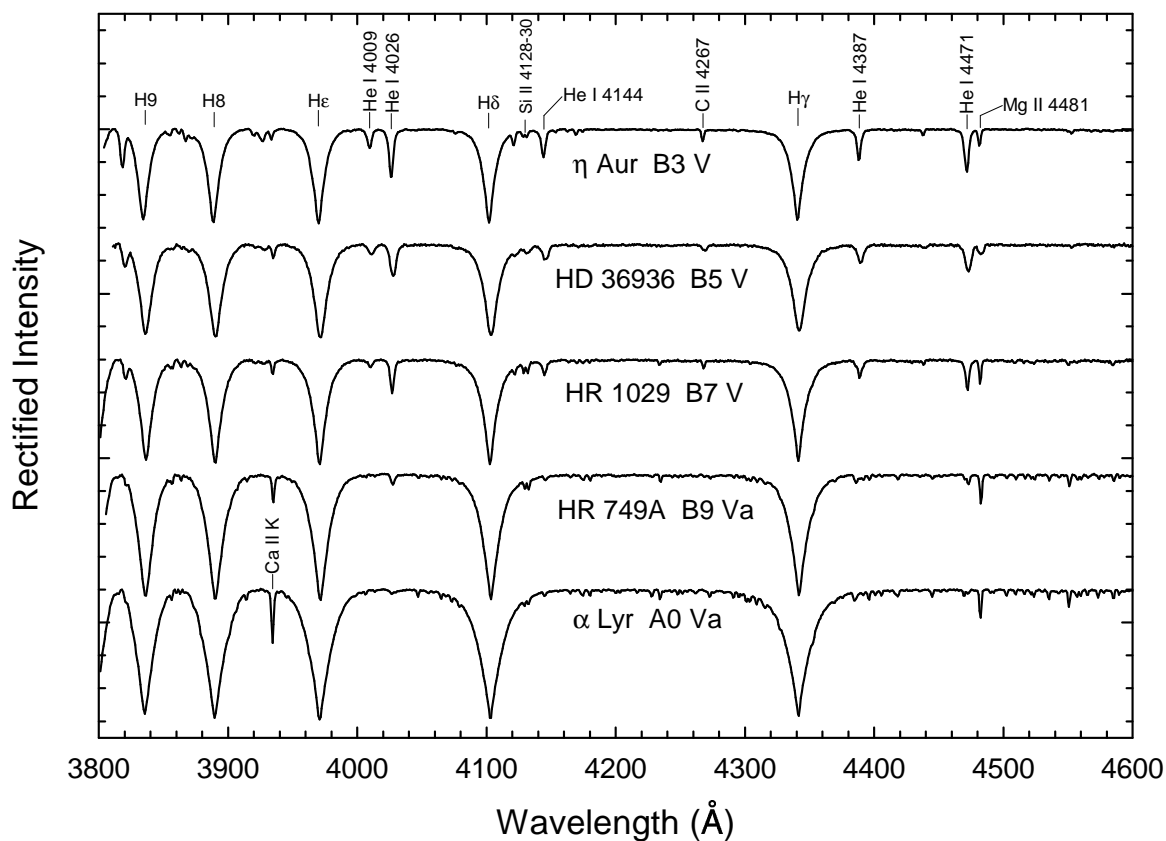
The Main Sequence B3 – A0

Figure 10: The main sequence from B3 to A0. Features useful in temperature classification are labeled. Note the increasing strength and width of the Balmer lines of hydrogen. Spectra from DSO.

As we move toward later (cooler) types, the helium lines continue to fade until they essentially disappear in spectra of this resolution (1.8Å) at a spectral type of about A0. Again, the ratio He I 4471/Mg II 4481 is useful in determining the spectral type in the late B-type stars. At A0, the Ca II K-line becomes a notable feature in the spectrum (in the B-type stars, the K-line is mostly interstellar).
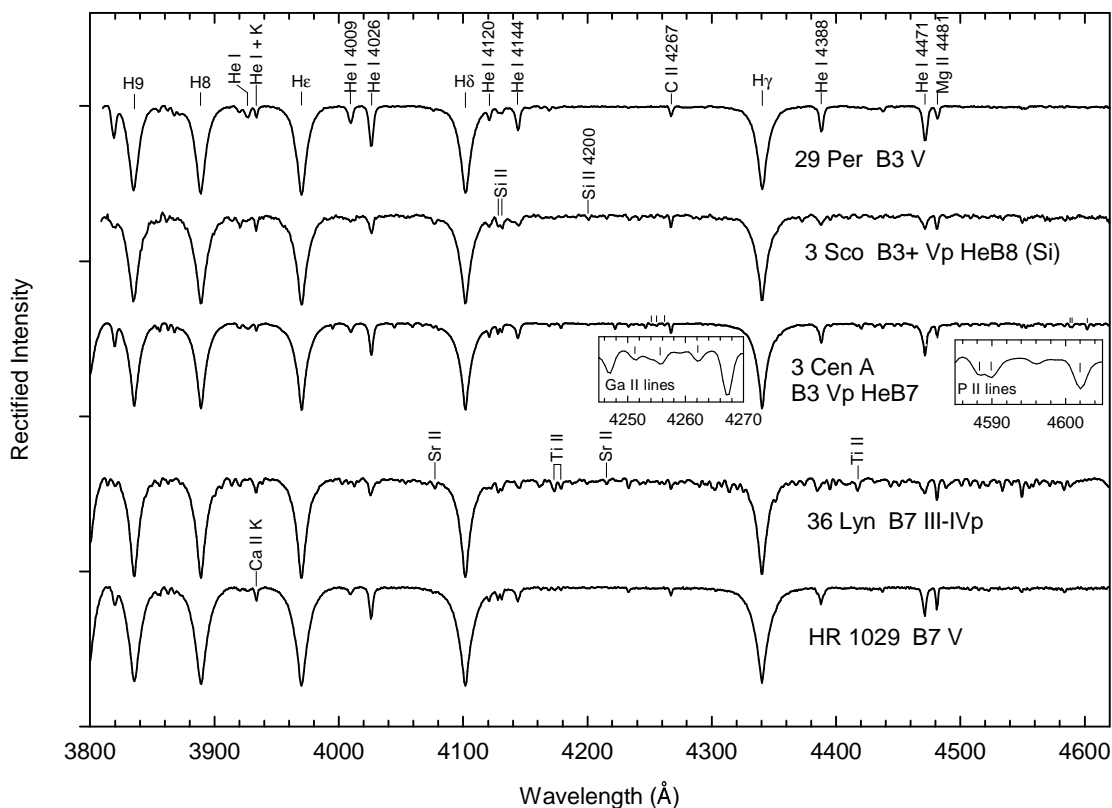
Helium-Weak B-type Stars

Figure 11: The spectra of three helium-weak B-type stars compared with two MK standards. Spectra adapted from the Paranal Observatory spectral library, from the Indo-US coudé-feed library and from DSO.

   The star, 3 Sco, is an excellent example of a helium-weak B-type star. The hydrogen lines of this star suggest a spectral type near B3 V whereas the strength of the helium lines suggests a spectral type of B8. This combination of criteria indicates the star is helium-weak, if we believe, as the $B - V$ color suggests, that the hydrogen lines are the best indicators of the effective temperature.

   Most helium-weak stars have spectral types of B3 and later, and thus this class has only a small spectral-type overlap with the helium-strong stars. Some helium-variable stars actually vary between a helium-weak and a helium-strong state.

   The figure above shows two other helium-weak stars. 3 Cen A also shows unusually strong P II and Ga II lines (see insets), and thus is an example of the class of PGa helium-weak stars. 36 Lyn shows strong lines of Sr II and Ti II, and is a prototype of the SrTi variety of helium-weak stars.
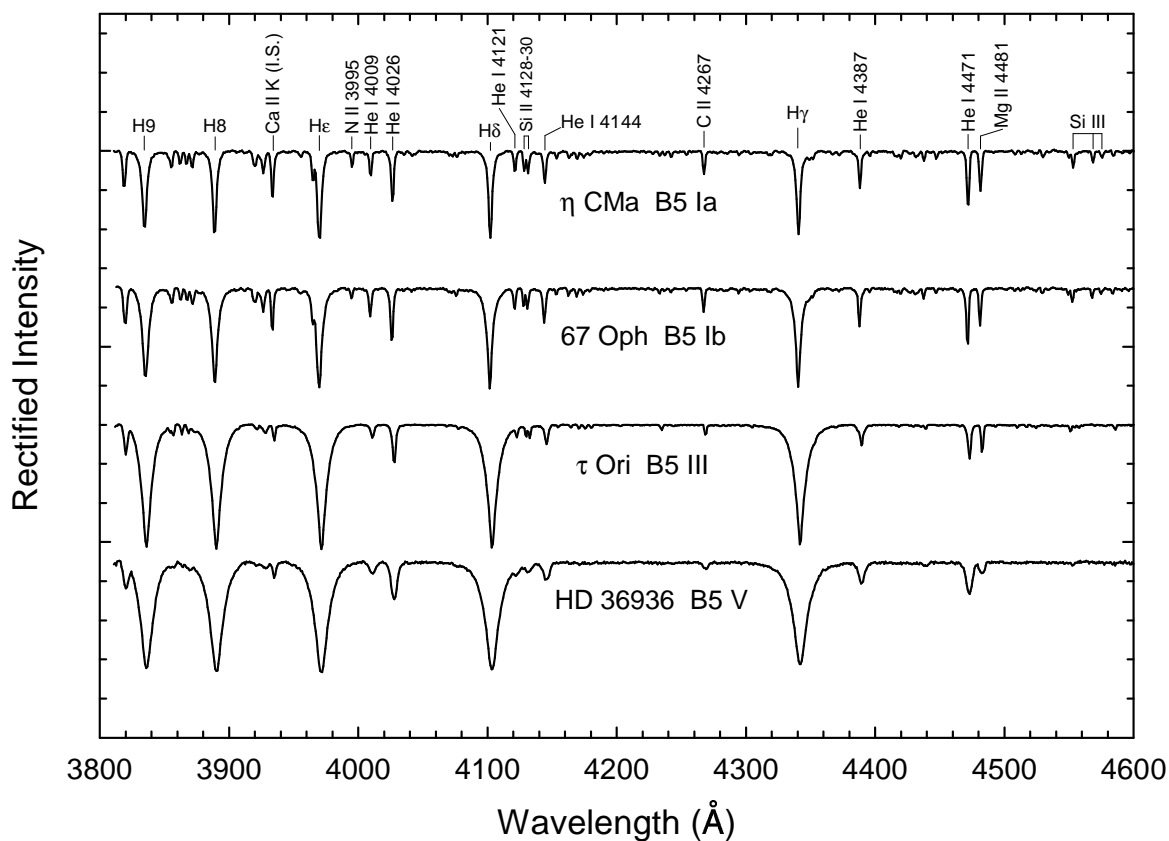
Luminosity Effects at B5

Figure 12: A luminosity sequence at B5. Spectra from DSO.

At B5 the primary luminosity criteria are the hydrogen lines which show a pronounced negative luminosity effect. The He I lines show little or no sensitivity to luminosity. However, note in the supergiant classes the strengthening of the Ni II $\lambda3995$ line and the Si III triplet ($\lambda4552$).
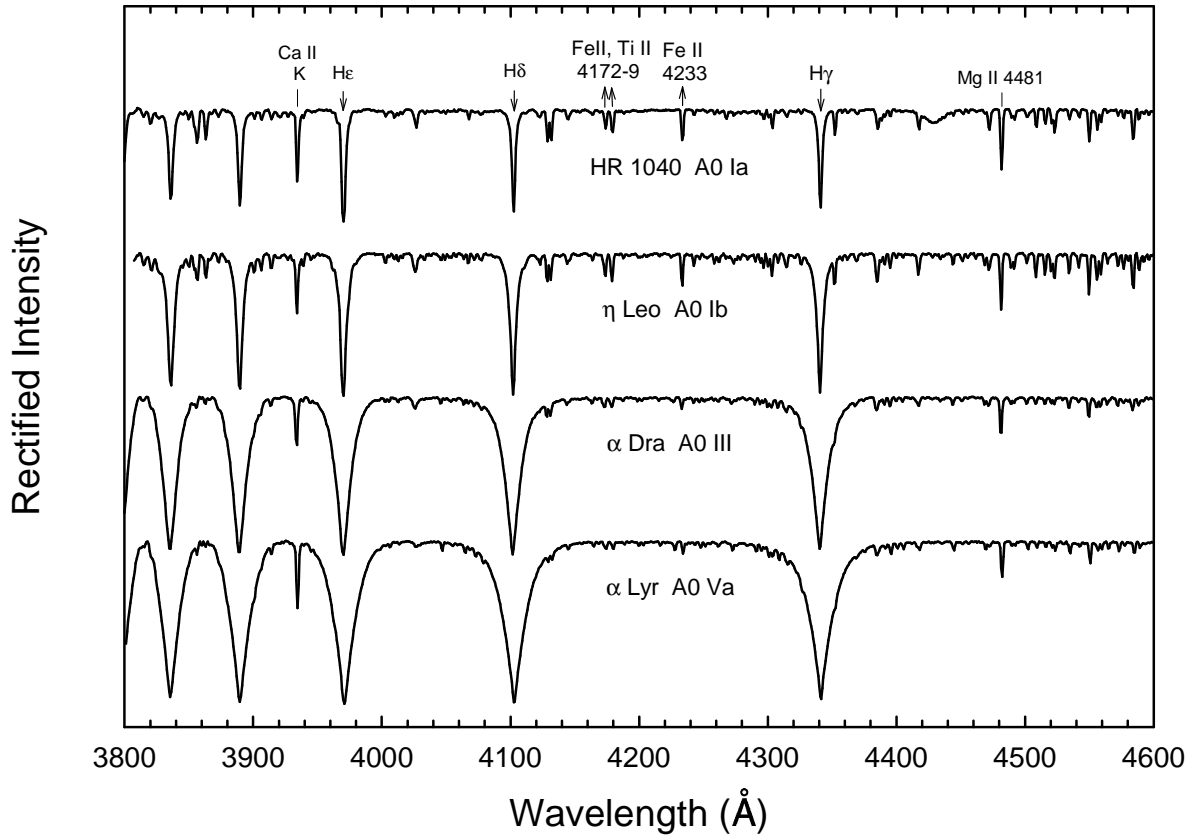
Luminosity Effects at A0

Figure 13: Luminosity effects at A0. Spectral features marked with upward arrows show a positive effect while the downward arrows indicate spectral features that show a negative luminosity effect. Spectral features marked with a line are insensitive to luminosity. Spectra from DSO.

Near a spectral type of A0, the primary luminosity criterion is the progressive widening and strengthening of the hydrogen lines with decreasing luminosity. Notice as well that certain lines of ionized iron (especially Fe II $\lambda4233$), certain blends of Fe II and Ti II (especially $\lambda\lambda4172$–8) and the Si II doublet ($\lambda\lambda4128 - 30$) are enhanced in the supergiants.
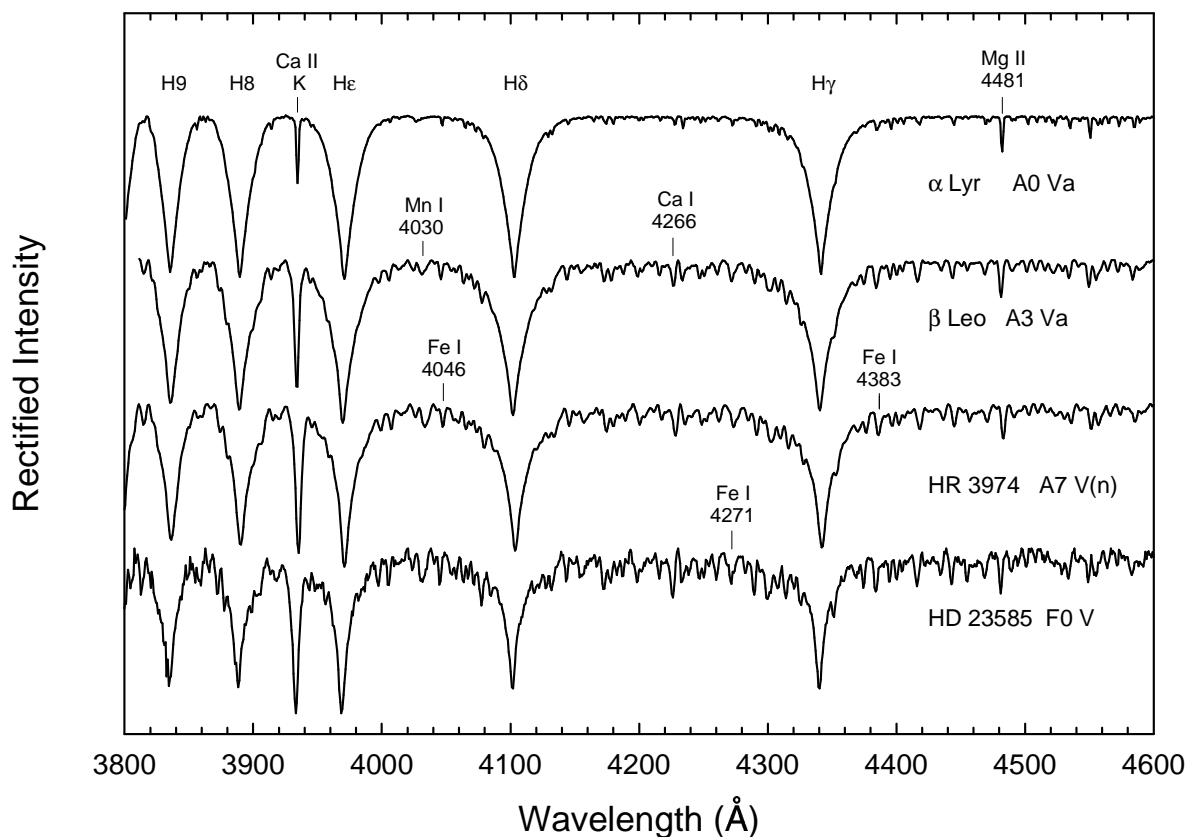
The Main Sequence A0 – F0

Figure 14: The main sequence from A0 to F0. The spectral features marked are useful in temperature classification of the A-type stars. Spectra from DSO.

The hydrogen lines reach a maximum in the A-type stars; on the main sequence this maximum is at A2. The Ca II K-line increases significantly in strength through the A-type stars, and its absolute strength, or, more usefully, its ratio with Hϵ or Hδ is a sensitive indicator of the temperature type, although one that is dependent on the metallicity. The general metallic-line spectrum also increases in strength through the A-type stars. These three criteria give a consistent temperature type in the normal A-type stars. Any disagreement between these three criteria indicates the star is peculiar in some way.
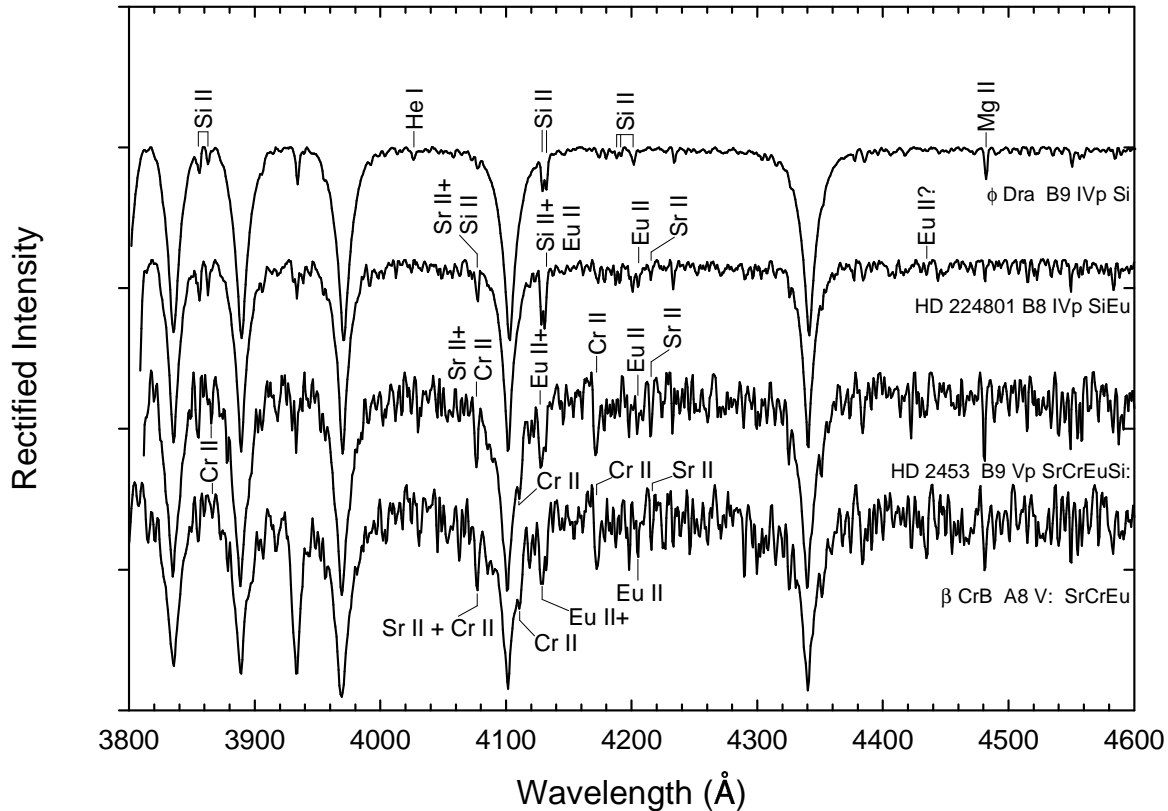
Peculiar A-type (Ap) stars

Figure 15: Illustrating four "typical" Ap stars, showing enhancements of Si, Cr, Eu and Sr. Note that many so-called Ap stars are actually B-type stars. The helium-weak nature of these stars has caused them to be erroneously classified as A-type stars. Spectra from DSO.

Ap stars are A-type (actually more commonly late B-type) stars that show significant enhancements of certain elements. The top spectrum (ϕ Dra) is that of a silicon Ap star; it shows enhanced lines of Si II, especially the $\lambda\lambda$4128-30 doublet. HD 224801 shows enhancements of both silicon and europium, with a hint of strontium. In HD 2453, strontium, chromium and europium are strongly enhanced. All three of these stars are actually late B-type stars. These stars have been traditionally classified as A-type stars because of the lack of He I lines in their spectra (although note ϕ Dra shows weak He I). Careful examination of the hydrogen-line profiles, however, helps to establish the correct spectral type. β CrB is considerably cooler, and shows strong enhancements of strontium, chromium and europium. All of the stars illustrated are so-called "classical Ap stars". All have strong magnetic fields.

Figure 16 shows the spectrum of a mercury-manganese star, α And. These stars show

greatly enhanced abundances of mercury and manganese, as well as a number of other elements.
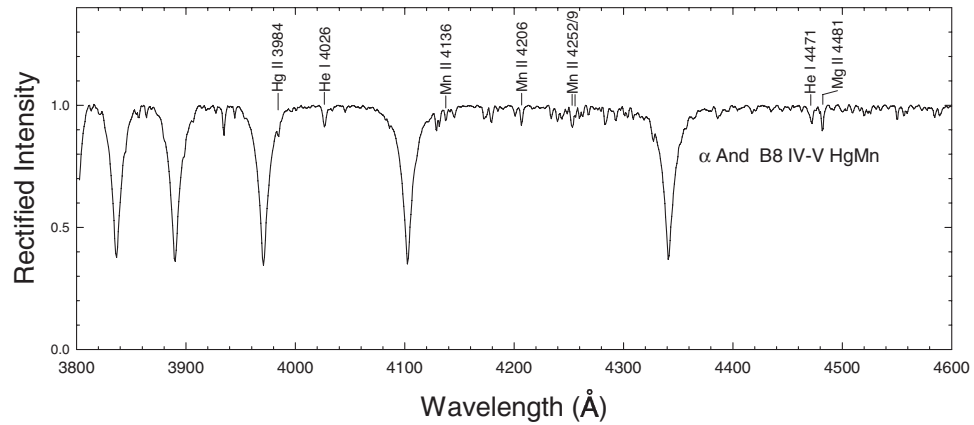

Figure 16: A spectrum of the mercury-manganese star α And. The most prominent lines of Hg II and Mn II are marked; the Mn II $\lambda 4252$ line may be blended with Ga II in this star. Spectrum from DSO.
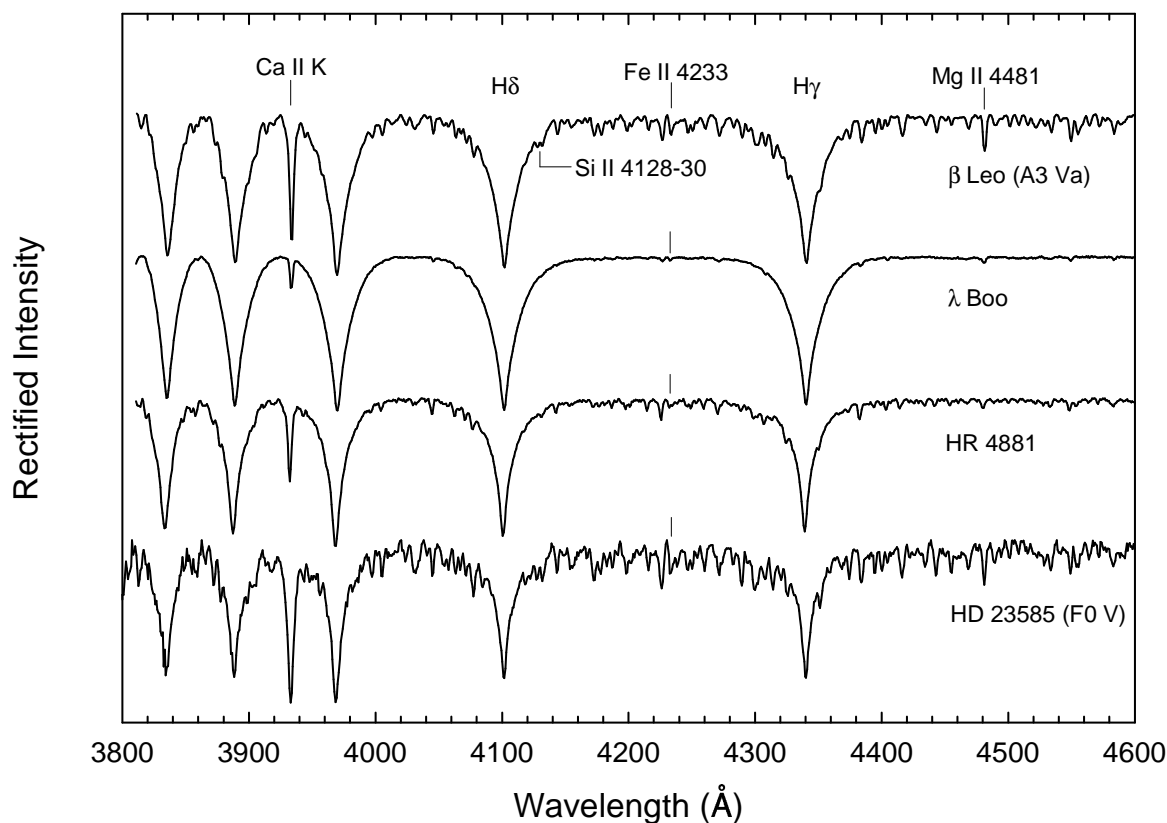
The λ Bootis stars

Figure 17: The spectra of two prototypical λ Bootis stars, λ Boo itself and HR 4881 compared with two MK standard stars. These standards were chosen because λ Boo has an A3 hydrogen-line type, and HR 4881 an F0 type. Note the outstanding weakness of the Mg II λ4481 line in the λ Boo stars. Spectra from DSO.

The λ Bootis stars are population I A-type stars that show marked underabundances of the iron-peak elements. Spectral analysis indicates that the most extreme of these stars can have metal deficiencies nearly 2 dex below the sun. Interestingly, they show nearly solar abundances of C, N, O, and S. These stars are recognized spectroscopically by their weak Mg II 4481 lines. However, since many peculiar types near A0 have weak λ4481 lines, to confirm a star as a λ Bootis star, it is also necessary to show that it is metal- weak. This can be done by first ascertaining the hydrogen-line type of the star, as the hydrogen lines are probably the best indicators of the effective temperature. Notice that the hydrogen lines of HR 4881 are best matched by the F0 V standard, HD 23585, whereas the metallic-line spectrum is weaker than the A3 standard. This clearly indicates that the star is metal-weak. The very broad hydrogen lines of the type star, λ Boo itself, indicate that it is an early A-type

star. Many λ Bootis stars are young; a few have been discovered in the Orion Association, including HD 37411, which is also a Herbig Ae/Be star. Many λ Bootis stars show evidence of circumstellar material, both dust and gas.
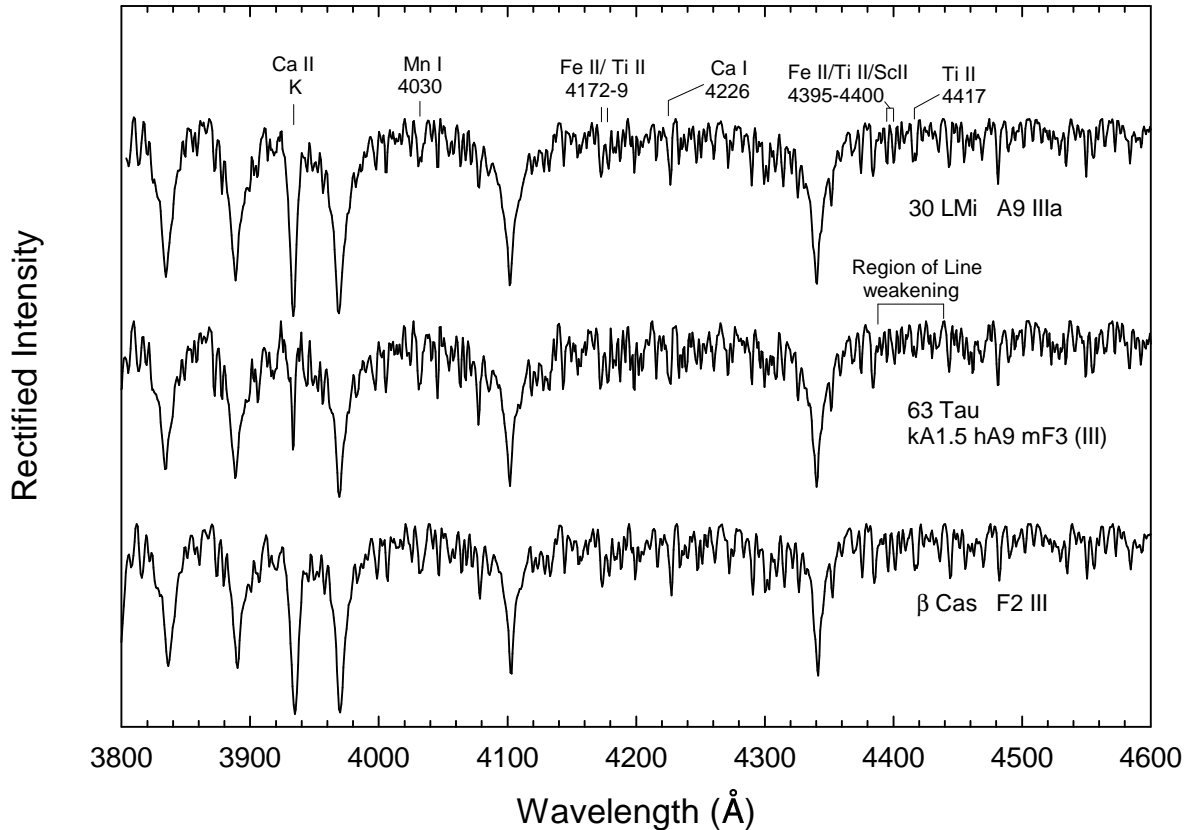
Metallic-line A-type Stars (Am stars)

Figure 18: The spectrum of an Am star, 63 Tau, compared with two normal stars, 30 LMi, an A9 giant, and β Cas, the MK F2 III standard. The hydrogen-line profiles of 63 Tau are an excellent match with 30 LMi, but the metallic-line spectrum looks slightly later than that of the F2 III. Note the weak K-line in 63 Tau. Spectra from DSO.

"Metallic-line" A-type stars, or, for short, "Am" stars, are defined as stars that show a difference between the K-line type and the metallic-line type. The star 63 Tau is a classic example of such a star. As can be seen in the figure, the Ca II K-line is weak (it is slightly weaker than that of the A2 standard), while the metallic-line spectrum is slightly stronger than that of β Cas. The hydrogen lines show an intermediate spectral type, estimated here as A9. The spectral type of this star is expressed, therefore, as kA1.5hA9mF3 (III). Notice that the Sr II 4077 line is enhanced in the Am star, and the Ca I 4226 line is weak. Many Am stars show the *anomalous luminosity effect* in which the luminosity criteria in certain spectral regions (in particular, the region from $\lambda\lambda 4077$–4200) may indicate a giant or even a supergiant luminosity, whereas other regions (such as the region of line weakening marked in the figure) indicate a dwarf luminosity or even lower.
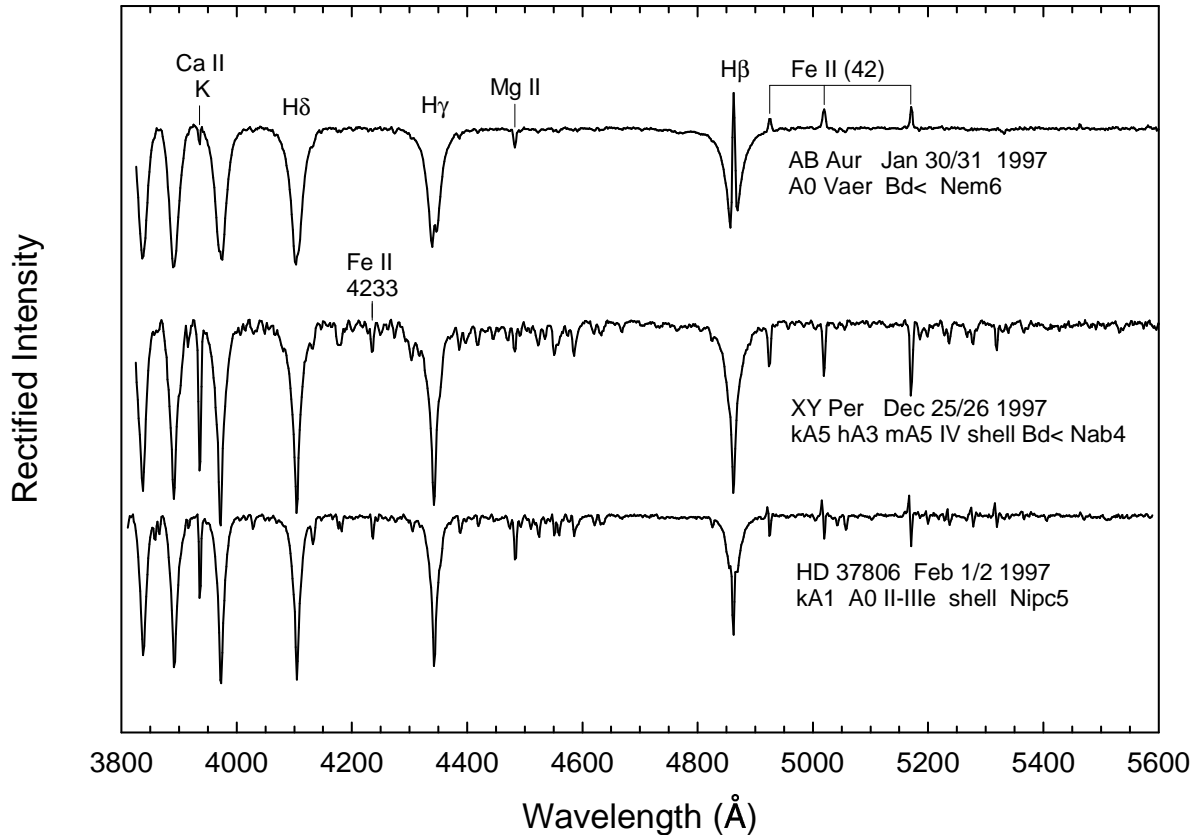
Herbig Ae (emission-line) stars

Figure 19: Spectra of three Herbig Ae stars. Note that lines of multiplet 42 of Fe II are in emission in AB Aurigae, in deep absorption in XY Per, and exhibit inverse P Cygni profiles in HD 37806. Both XY Per and HD 37806 show pronounced shell features, including a strong Fe II $\lambda4233$ line. These 3.6Å resolution spectra were obtained at DSO.

Herbig Ae stars generally show emission in the Hα line (outside of the spectral range of most of the spectra used in this atlas), and quite often emission in Hβ and even Hγ . Many Ae stars are still contracting to the main sequence, and are thus either still surrounded by remnants of their stellar cocoons, or have developed massive stellar winds.

Recently, Gray & Corbally (1998) have devised an extension of the MK Classification System to the Herbig Ae-type stars. This system, in addition to the usual MK-type, utilizes indices to indicate emission or stronger than normal absorption in lines of the Fe II (42) multiplet, the strength of the Balmer decrement, and characteristics of the emission in the Hβ line. The three stars illustrated here demonstrate that system. The extended spectral type consists of a normal MK type along with an indication of the nature of the Balmer line emission. An "e" indicates strong emission in the Hβ line, (e) indicates marginal or weak

emission, and an "r" or "b" indicates whether this emission is shifted to the red or blue of the photospheric line. The strength of the Balmer decrement is indicated by the symbols $<, \leq, =, \geq, >$ for weak, somewhat weak, normal, somewhat strong, and strong. The nature of the emission and/or absorption, plus the strength relative to the normal absorption strength of the relevant standard of the lines of the Fe II (42) multiplet are indicated with the N index. Nem indicates these lines are in emission, Nab that they are in stronger than normal absorption, and Npc and Nipc indicate P Cygni and inverse P Cygni profiles in these lines.

The spectral types of these Herbig Ae stars can change quite dramatically on time scales of a few days. As a consequence, the spectral types of these stars should always be accompanied by a date.
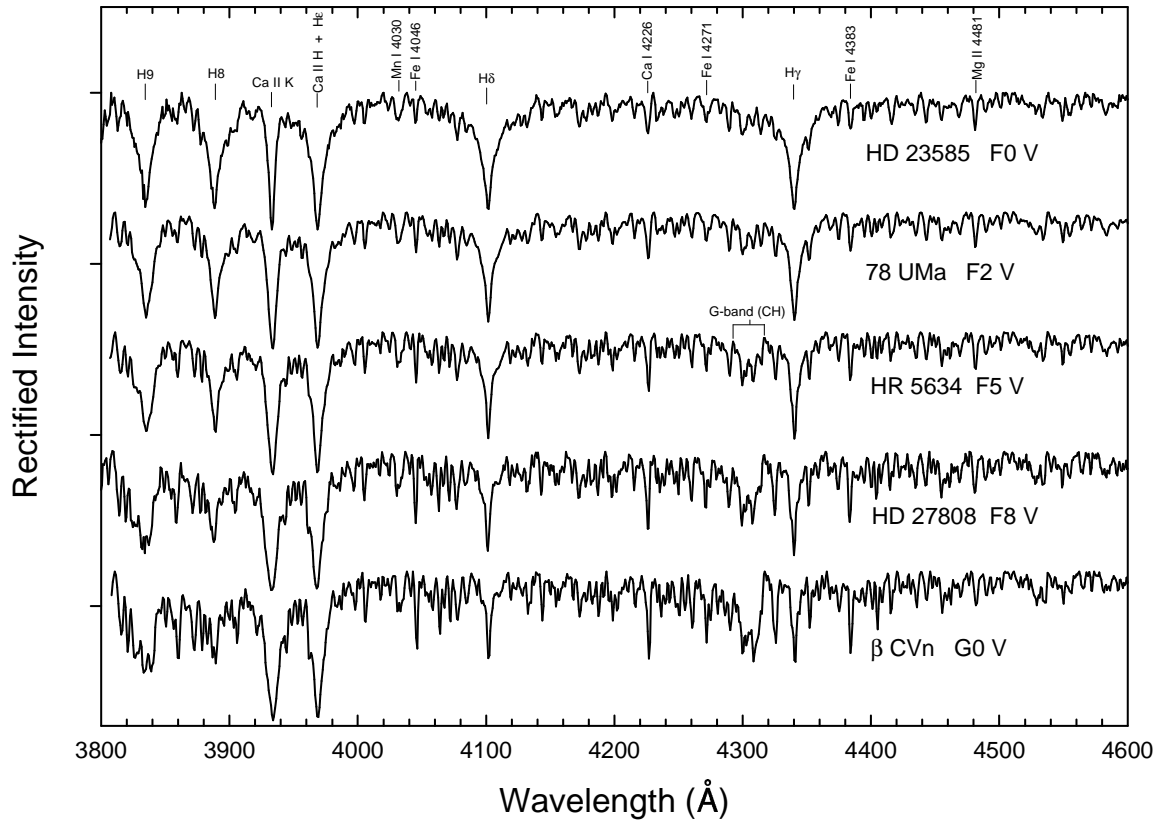
The Main Sequence F0 – G0

Figure 20: A temperature sequence for main-sequence F-type stars. Features useful in the temperature classification of the F-type stars are marked. Spectra from DSO.

The hydrogen lines continue to weaken through the F-type stars, and the Ca II K-line strengthens, although it becomes essentially saturated by the late F-type stars. The general strength of the metallic-line spectrum (note especially the features marked on the illustration) grows dramatically. Around F2, depending upon the resolution of the spectrum, the G-band makes its first appearance. The G-band is a molecular band, composed of thousands of closely spaced lines due to the diatomic molecule CH.
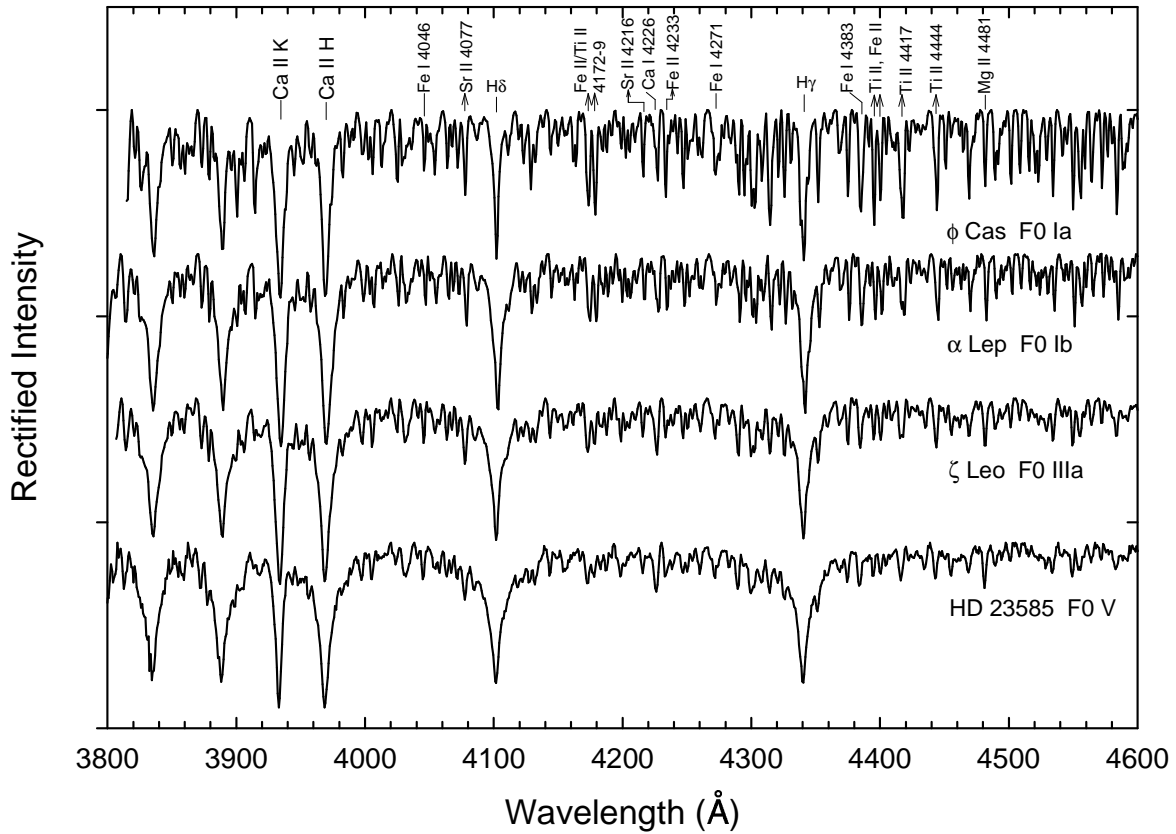
Luminosity Effects at F0

Figure 21: Luminosity effects at F0. Spectral features marked with upward arrows show a positive luminosity effect; those marked with a line are relatively insensitive to luminosity. Note that the hydrogen lines show only a weak negative luminosity effect. Spectra from DSO.

By F0, the hydrogen lines have lost most of their sensitivity to luminosity. Note, however, that they can still be used to distinguish the supergiant classes from lower luminosities. Near F0, the luminosity class is estimated from the strength of lines due to ionized iron and titanium. Excellent luminosity-sensitive features include the Fe II, Ti II double blend at $\lambda\lambda4172$–8, and similar blends at $\lambda\lambda4395$–4400, $\lambda4417$ and $\lambda4444$. The strength of these blends are usually estimated with respect to other less luminosity sensitive features, such as Ca I $\lambda4226$, Fe I $\lambda4271$ and Mg II $\lambda4481$.
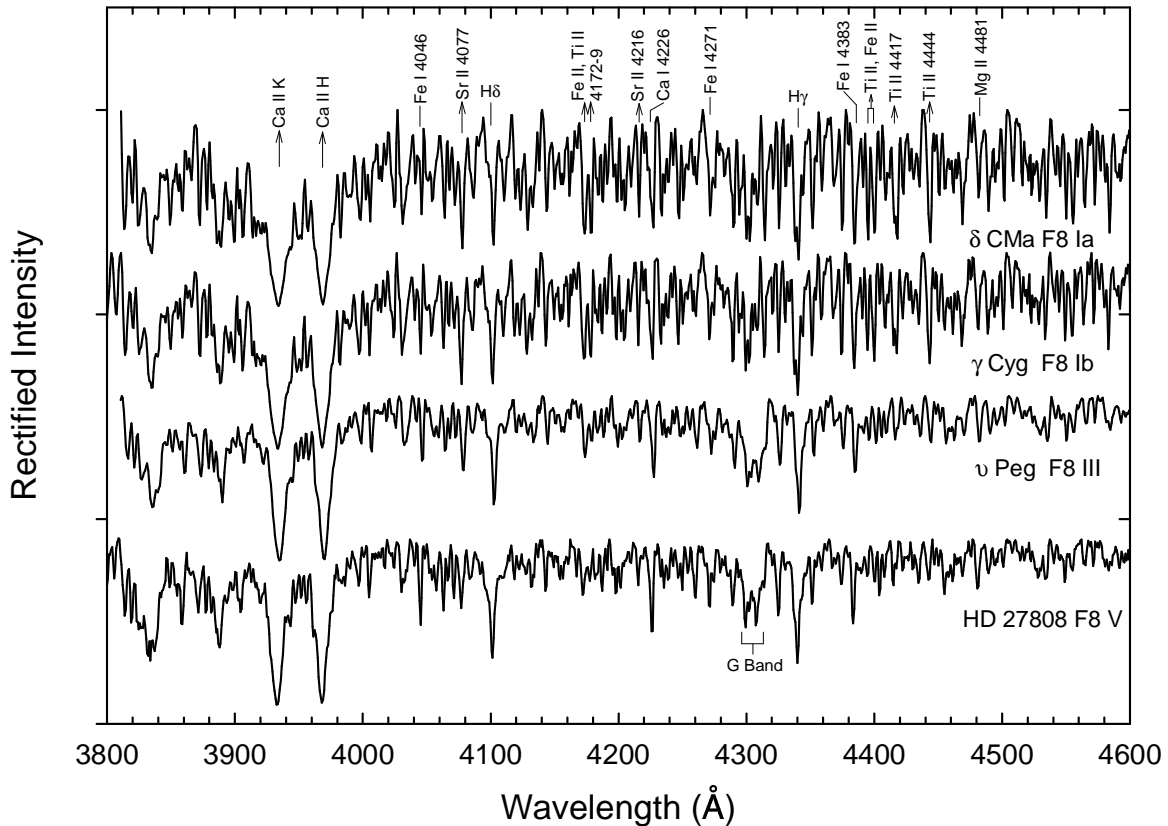
Luminosity Effects at F8

Figure 22: Luminosity effects at F8. Spectral features marked with upward arrows show a positive luminosity effect; those marked with a line are relatively insensitive to luminosity. Note the change in the morphology of the G-band (marked below the F8 V spectrum) with luminosity. Spectra from DSO.

By F8, the hydrogen lines have lost all sensitivity to luminosity, and it is now necessary to rely solely on lines and blends of ionized species. The luminosity sensitive features are essentially the same as at F0, except that at F5 and later types, the Sr II $\lambda\lambda 4077$ and 4215 lines show excellent sensitivity to the luminosity. Note, however, that these lines may be enhanced in chemically peculiar stars, such as the barium dwarfs. Also note that at F5 (and later types), the Ca II K-line shows a slight positive sensitivity to luminosity, in the sense that it becomes slightly broader in the more luminous stars.
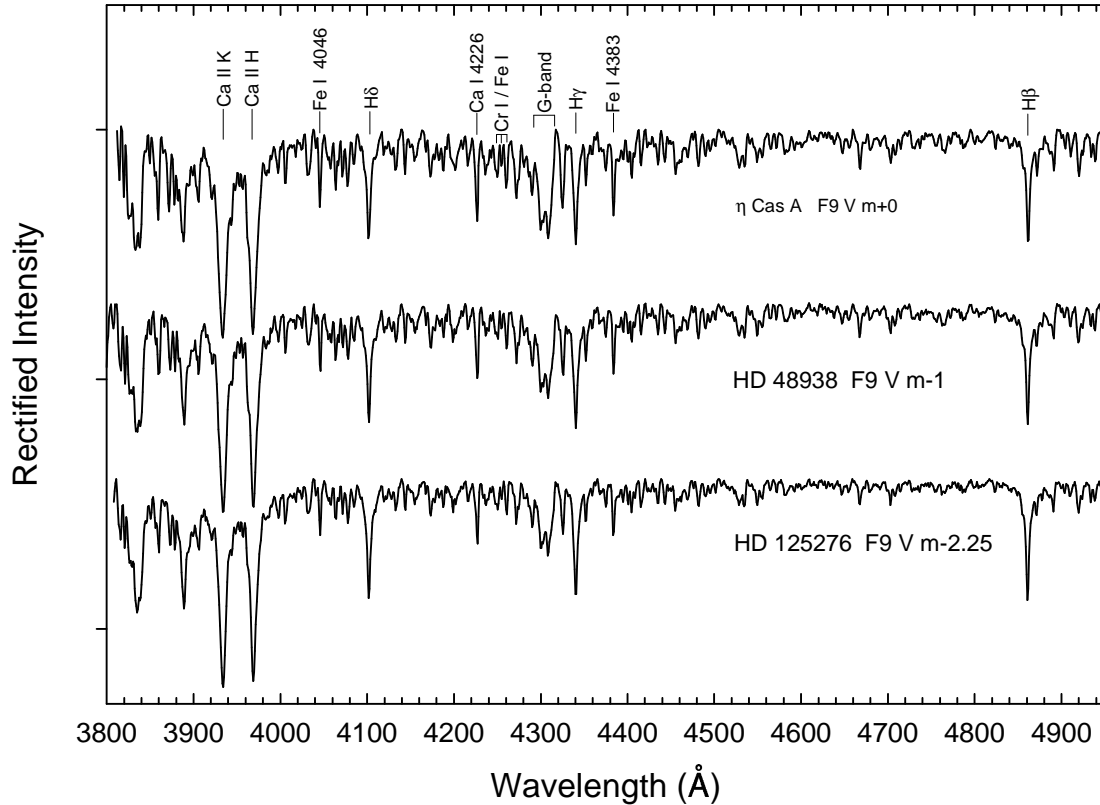
Metal-weak F-type Stars

Figure 23: A metallicity sequence of F9 main-sequence stars classified on Gray's 1989 system. These spectra were obtained on the Steward Observatory 90" Bok telescope, and have a slightly lower resolution than the 1.8Å resolution DSO spectra in many of the previous figures.

Main-sequence stars with a wide range of metallicites can be found in the solar neighborhood. Illustrated here are three stars classified on Gray's 1989 extension of the MK system. This extension accommodates metal-weak stars of the thick disk and halo. The degree of metal deficiency is indicated on this system with an "m" index, which is well correlated with [Fe/H] measurements in the literature.
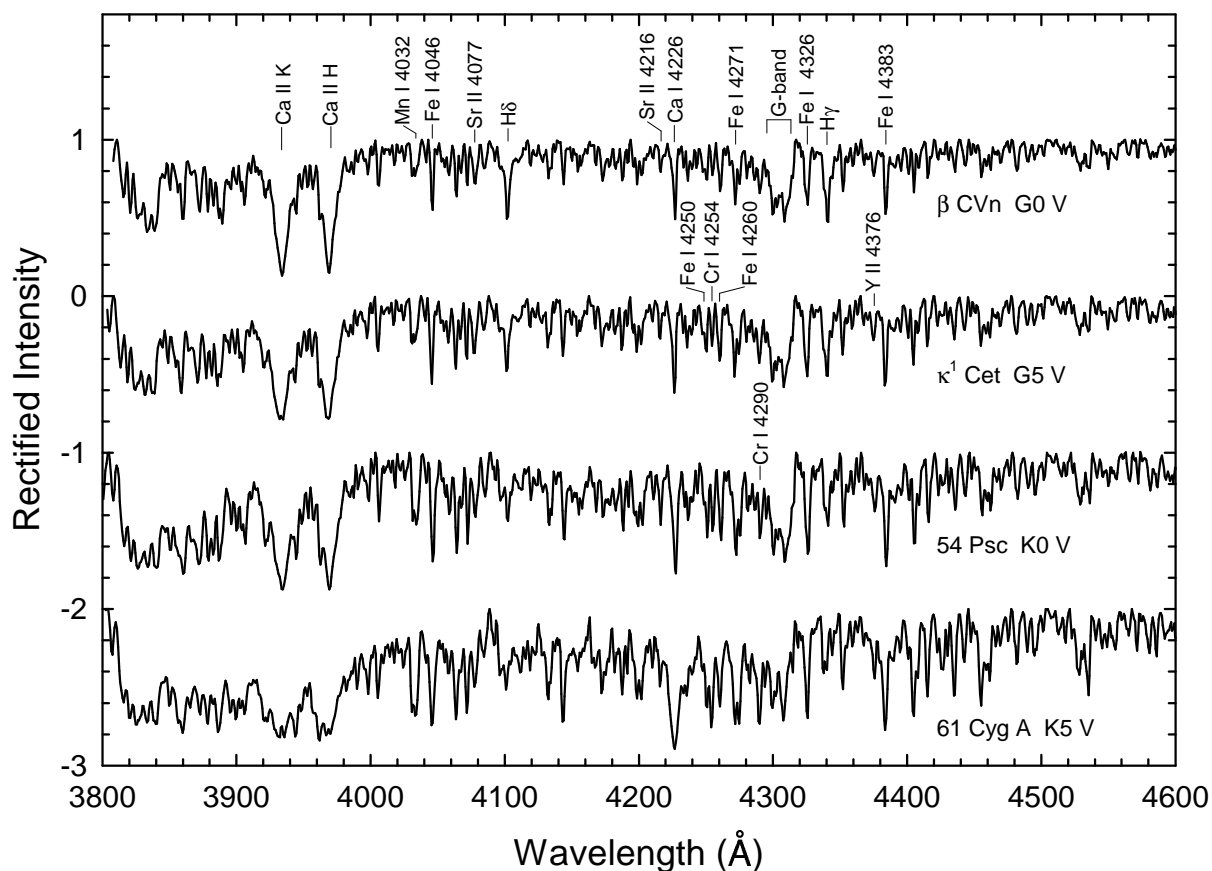
Main Sequence G0 – K5

Figure 24: A temperature sequence for main-sequence stars from G- to mid-K types. Features useful in the temperature classification of these stars are marked. DSO 1.8Å resolution spectra.

Later than G0 along the main sequence, the hydrogen lines continue to fade, while the strength of the general metallic-line spectrum continues to increase. The G-band also increases in strength until the early K-type stars (about K3), and then begins to fade. The Ca I 4226 line grows gradually in strength until the early K stars, and then becomes dramatically stronger by mid-K. The ratios Fe I $\lambda 4046$/Hδ and Fe I $\lambda 4325$/Hγ are useful in estimating the temperature type, reversing at a spectral type near G8. Unfortunately, these ratios are not reliable in metal-weak or metal-strong stars. The temperature type may be estimated with precision, even in metal-weak stars by using the ratio of the Cr I $\lambda 4254$ resonance line with the two neighboring Fe I subordinate lines at $\lambda 4250$ and $\lambda 4260$. Notice that the Cr I line becomes stronger in ratio with the two flanking higher-excitation Fe I lines, being clearly stronger than both by K5.

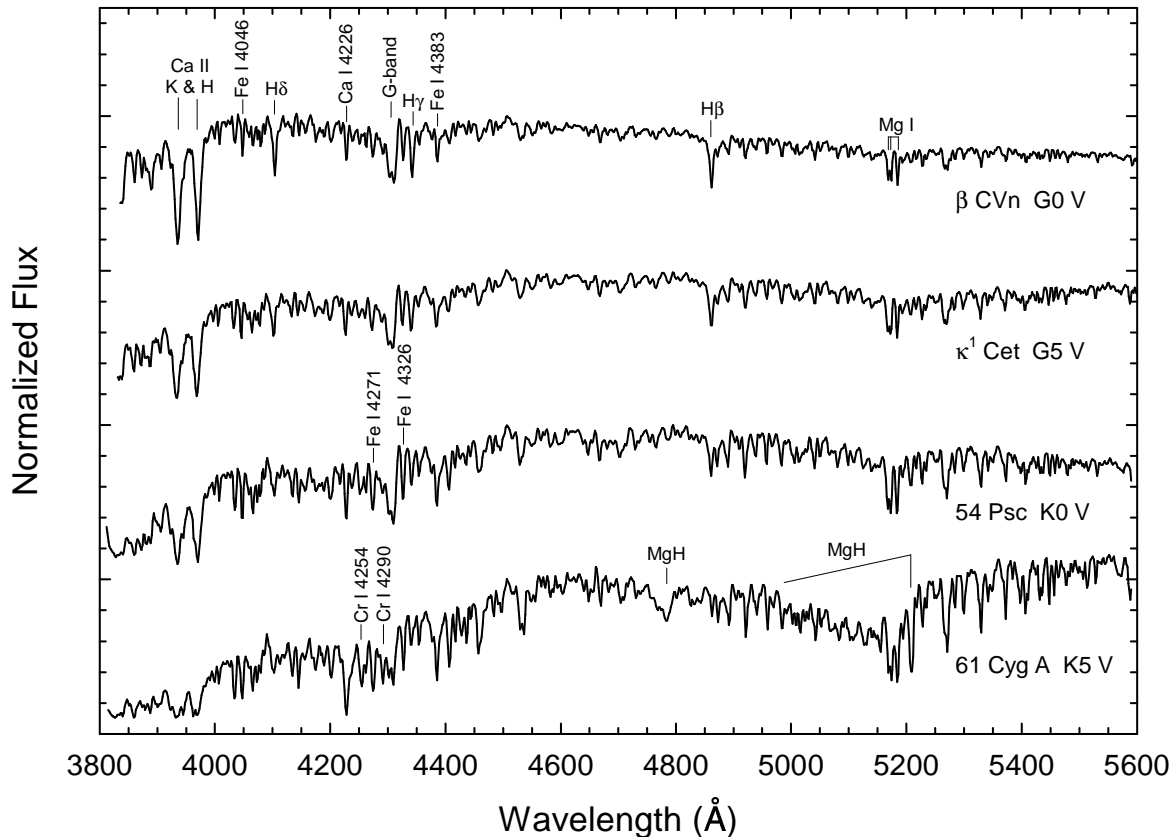# Main Sequence G0 – K5, 3.6Å Resolution spectra

Figure 25: The same temperature sequence for main-sequence stars illustrated in Figure 24, but with lower resolution (3.6Å as opposed to 1.8Å spectra) normalized flux spectra. Features useful in the temperature classification are marked. DSO 3.6Å resolution spectra.

This figure reproduces the temperature sequence of the previous figure, but employs "normalized-flux" spectra instead of "rectified intensity" spectra in which the continuum points are normalized to unity. The flux representation is advantageous in late-type stars because line blanketing in these spectra is so great that there are no true continuum points. These spectra also have a lower resolution (3.6Å) than in the previous figure (1.8Å), but show a wider spectral range, also often of advantage in classifying late-type stars. The temperature criteria noted in the previous figure can also be used in these spectra, although the resolution here is too low to resolve clearly the Cr I $\lambda 4254$ line from the neighboring Fe I lines at $\lambda 4250$ and $\lambda 4260$. However, the broader spectral range brings other temperature criteria into play. Note the development of the MgH feature at 4780Å. This feature first appears at a spectral type of K4. The prominent wedge-like continuum depression in the vicinity of the Mg I

triplet ($\lambda\lambda$5167, 5172, and 5184), also partially due to MgH, is a distinctive feature of dwarfs later than K2. The morphology of the line spectrum in the vicinity of Hβ is a sensitive indicator of the temperature-type, with the progressive fading of the Hβ line. However, this criterion should be used only for solar-abundance stars.
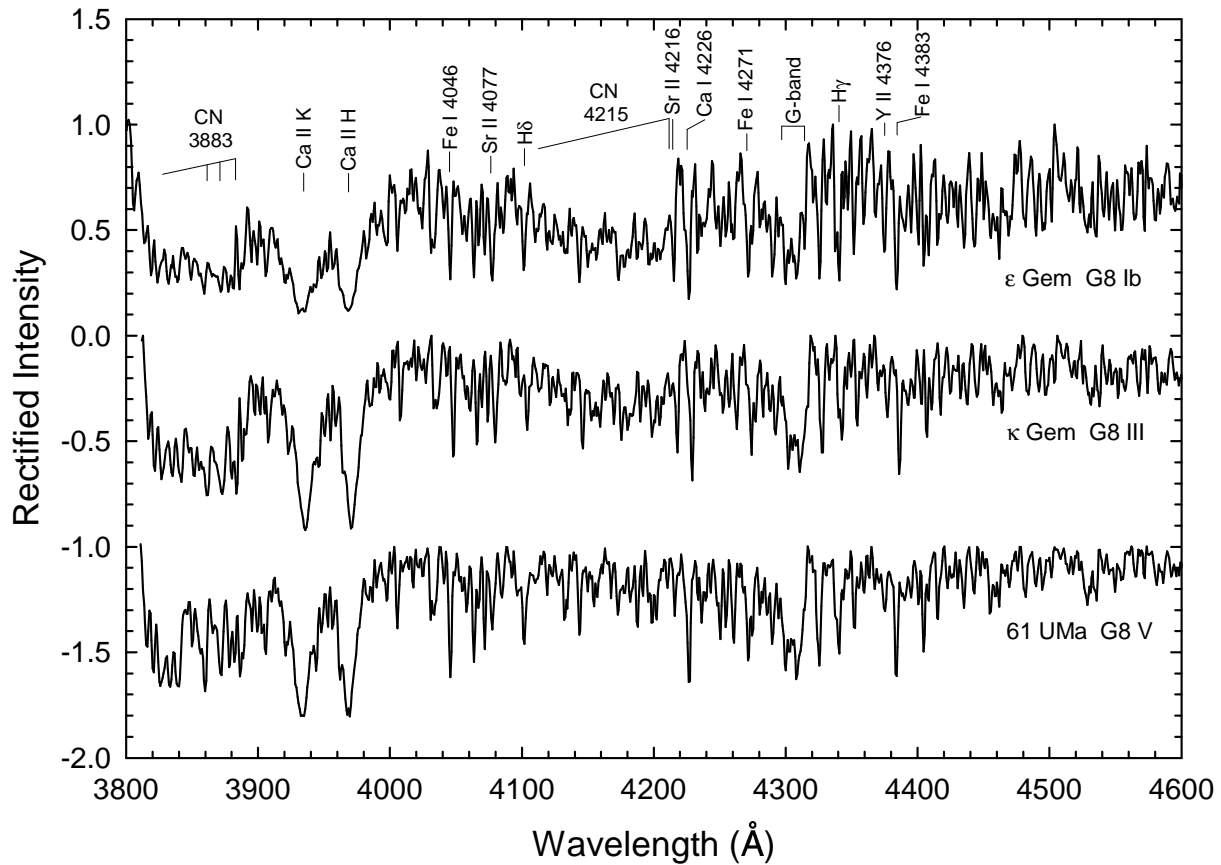
Luminosity Effects at G8

Figure 26: Luminosity effects at G8. Principal features are marked. The two CN bands show a positive luminosity effect, while the ratio of the Y II λ4376 line to Fe I λ4383 is particularly useful since it is the most metallicity independent. Spectra from DSO.

The ratios of Sr II λ4077 to nearby iron lines (Fe I $\lambda\lambda$4046, 4063, and 4071) remain sensitive to luminosity. The violet-system CN bands, with bandhead at 4215Å, visible in the supergiant and giant spectra as a concavity in the continuum, show a strong sensitivity to luminosity. Notice as well that the Ca II K and H lines show extremely broad damping wings in the supergiant class. But the criterion affording the greatest discrimination in the luminosity classes is the ratio of the Y II λ4376 line to Fe I λ4383.
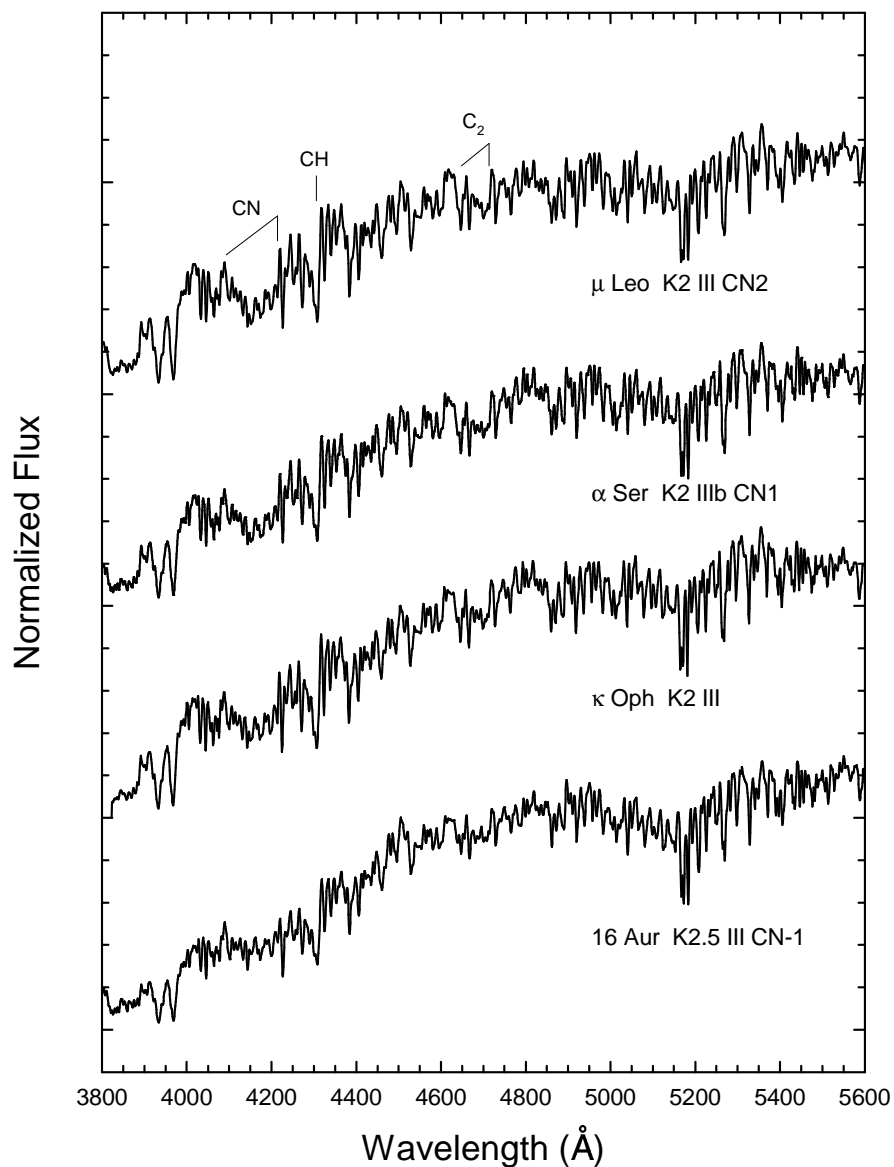
K Giants with Unusual CN-band Strengths

Figure 27: K Giants with unusual CN and C_2 band strengths. DSO 3.6Å resolution spectra.

A number of G and K-type giants show either strong or weak molecular bands involving carbon. Illustrated here are a number of K2 III stars showing CN and C_2 bands of different strengths, along with the K2 III standard, κ Oph. The luminosities of such chemically peculiar stars are determined using criteria independent of these bands.

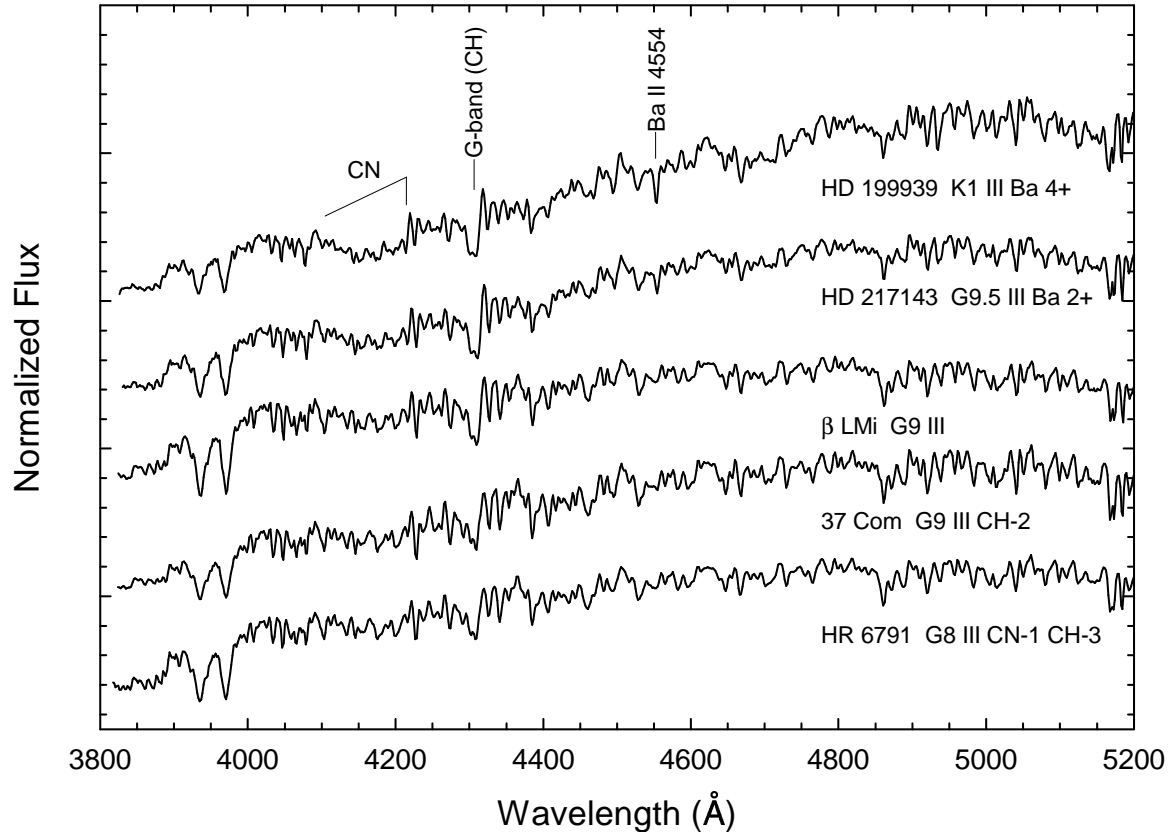# More Late-G Giants with Abundance Peculiarities

Figure 28: Late-G giants with abundance peculiarities. DSO 3.6Å resolution spectra.

In this figure are illustrated a number of late-G, early-K giant stars with abundance peculiarities. HD 199939 is a barium giant star, showing an exceptionally strong Ba II resonance line at $\lambda 4554$. HD 217143 is a milder barium giant. β LMi is the G9 III MK standard. 37 Com is a G9 III with an abnormally weak G-band, but quite normal CN 4215 band. HR 6791 is a G8 III with weak CN bands and a weak G-band. Almost all barium stars are members of binary systems in which the companion is a white dwarf. It is believed that the enhanced abundances of s-process elements, such as barium, were gained from the companion star when it was on the *Asymptotic Giant Branch* (AGB). The mass transfer came about either through Roche-lobe overflow or wind accretion. The *s*-process elements are the result of slow neutron capture, which occurs only at advanced stages of nuclear burning.
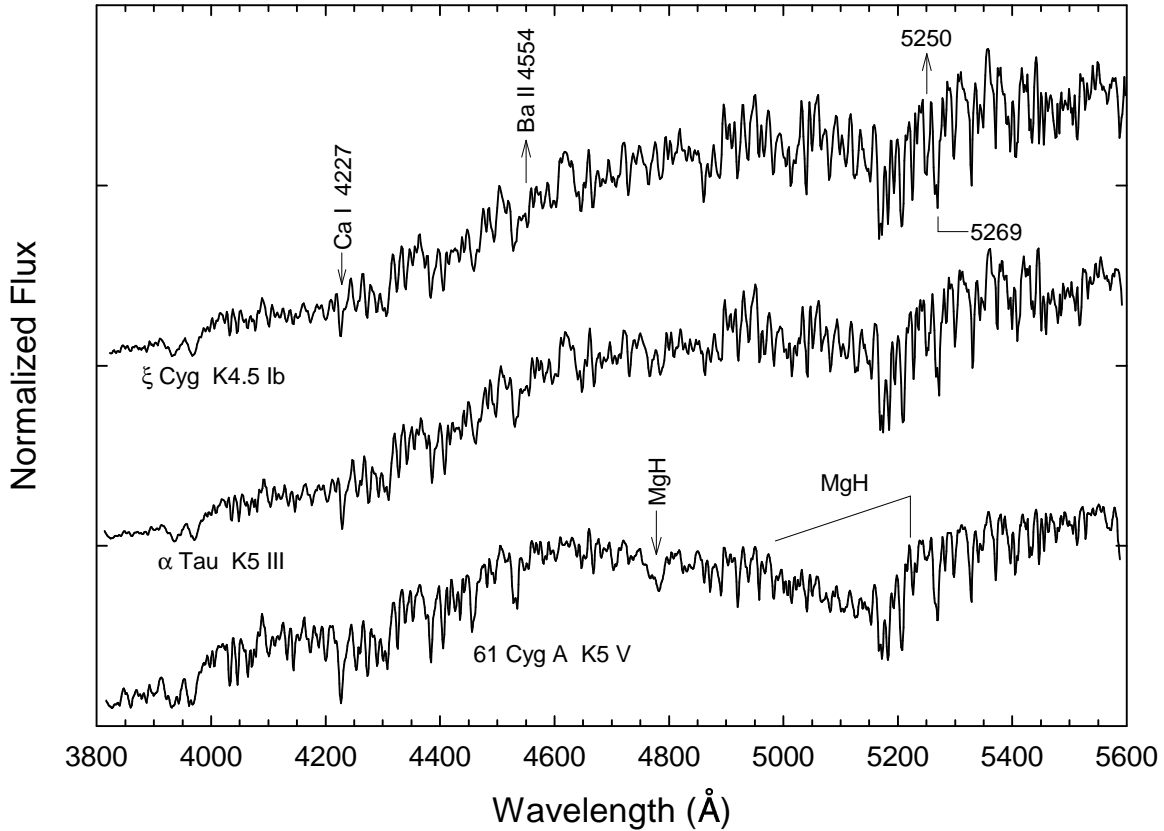
Luminosity Effects at K5

Figure 29: Luminosity effects at K5. DSO 3.6Å resolution spectra.

The negative luminosity effect in the Ca I $\lambda4226$ line is an important luminosity criterion in the K5 stars. The Ba II $\lambda4554$ resonance line shows a positive luminosity effect, but classifiers should be aware that this line may be enhanced in chemically peculiar K-type giants. The MgH bands show a negative luminosity sensitivity; the strength and the morphology of the narrow MgH feature near 4770Å is especially useful; it can be ratioed with Hβ and neighboring metal lines. The line ratio $\lambda5250/\lambda5269$ is as well an excellent luminosity criterion in the K5 stars. The $\lambda5250$ feature is a pressure sensitive blend involving a number of intersystem Fe I lines.
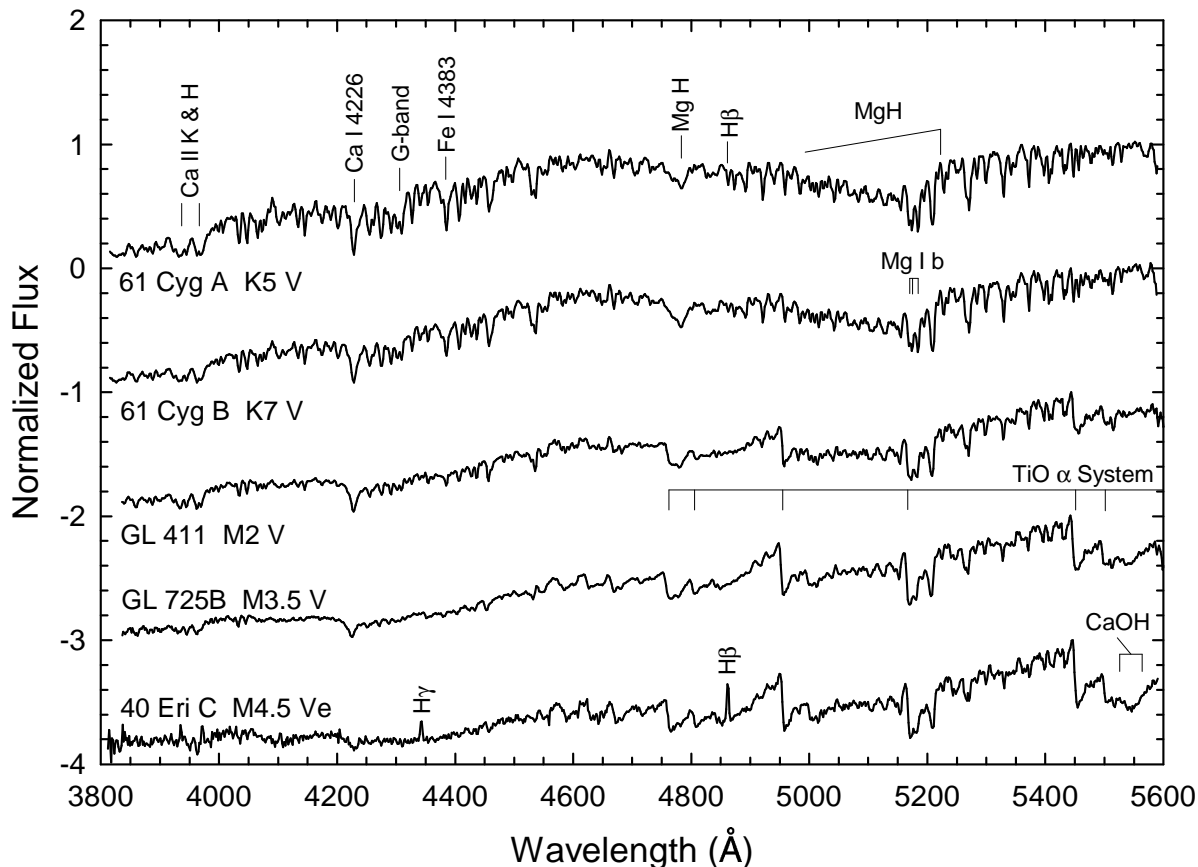
Main Sequence K5 – M4.5

Figure 30: A temperature sequence of main sequence stars from late-K to mid-M with the principle spectral criteria labelled. DSO 3.6Å resolution spectra.

This figure uses 3.6Å resolution spectra to take advantage of their broader spectral coverage. In addition, the ordinate in this figure is in terms of "flux" instead of "rectified intensity", so that the change in the shape and slope of the continuum can be seen as a function of spectral type. In the K-type dwarfs, the spectral type may be estimated from the ratio of Ca I $\lambda 4226$ to Fe I $\lambda 4383$, in the sense that Ca I/Fe I grows toward later types. In addition, K5 and K7 dwarfs may be distinguished by 1) the ratio of the MgH feature at 4780 to neighboring lines and 2) the first subtle indications of TiO in the K7 dwarf. By M0, bands due to TiO begin to be significant features in the spectrum, and these strengthen quite dramatically toward later types; by M4.5 they dominate the spectrum. To exclude the possibility of systematic errors in metal-weak stars, ratios of TiO band strengths should be employed. Notice as well the development of the MgH feature at 4780Å. It begins in the mid-K-type dwarfs as a pointed tooth- like absorption feature, which then becomes progressively more flat-bottomed as a nearby TiO band grows in strength. A band of CaOH, a tri-atomic

molecule, makes its first appearance at about M3, and contributes to a strong absorption feature by M4.5. Notice that Hβ is in emission in the M4.5 star; many M dwarfs have active chromospheres and exhibit strong flares many times more energetic than solar flares. One of the manifestations of this is emission in the hydrogen lines.
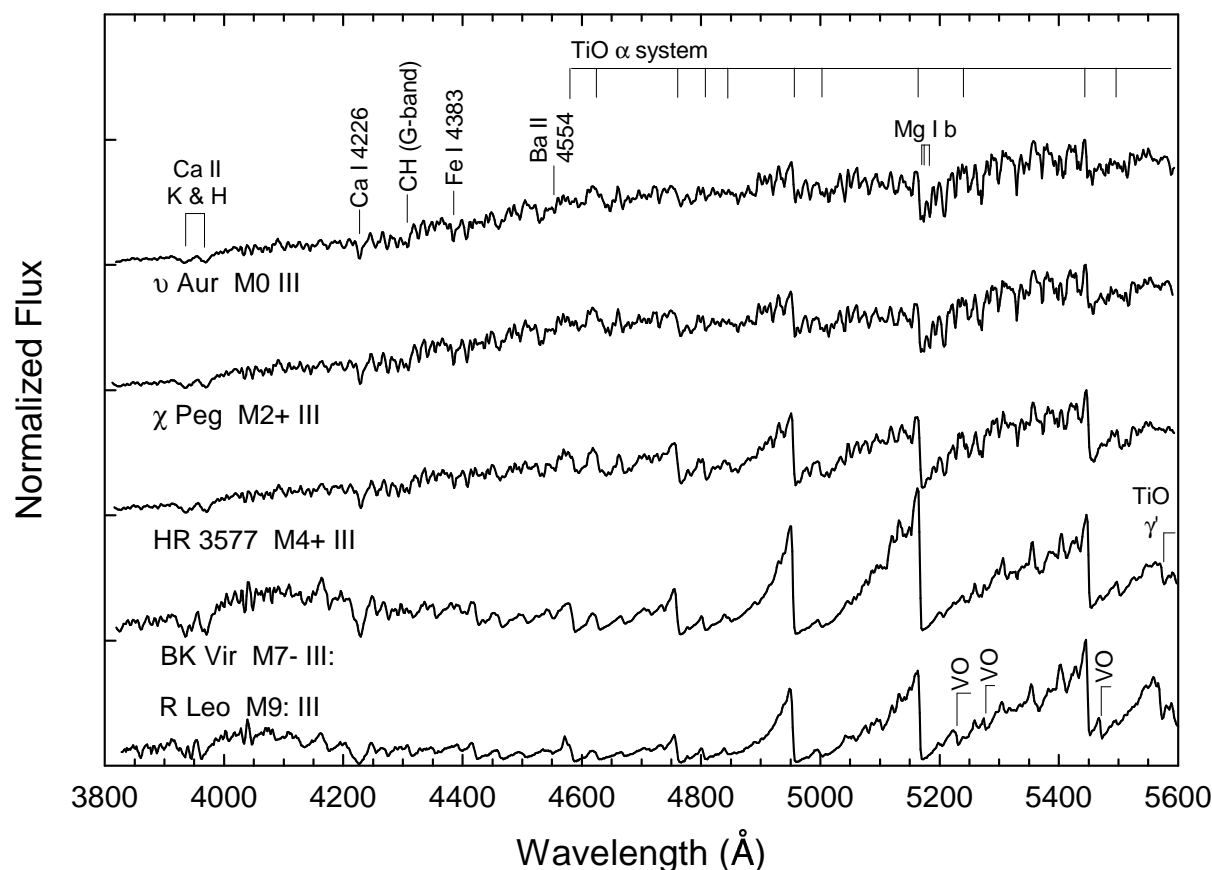
An M-Giant Temperature Sequence

Figure 31: A temperature sequence for M giants. DSO 3.6Å resolution spectra.

Temperature classification of the M-type giants is based primarily on the increasing strength of the TiO bands. At K7, the TiO $\lambda 5448$ bandhead can just barely be detected; after M3 the strongest bands become saturated, and the temperature type is assigned on the basis of the strength of the fainter bands.

To avoid complications due to abundance or population effects or the "veiling" phenomenon in which the spectral features appear washed out (this can be a particular problem in the variable M-type stars, such as the Mira variable stars), it is best to judge the spectral type on the basis of the ratios of the strengths of these bands. In particular, it is useful to consider ratios of the orange-red γ' system of TiO with bands of the blue-green α system. Only the bluest band of the γ' system is visible in these spectra. Note the appearance of VO bands in the M9 giant.

The metallic lines reach a maximum strength in the early M-type stars; in later types the successively stronger absorption due to TiO begins to reduce the line strengths in the spectral

region illustrated here. The Ca I $\lambda4226$ line, however, continues to increase in strength in the giants, especially after M5. Note the violet (near 4100Å) flux "bump" in the two latest spectra.
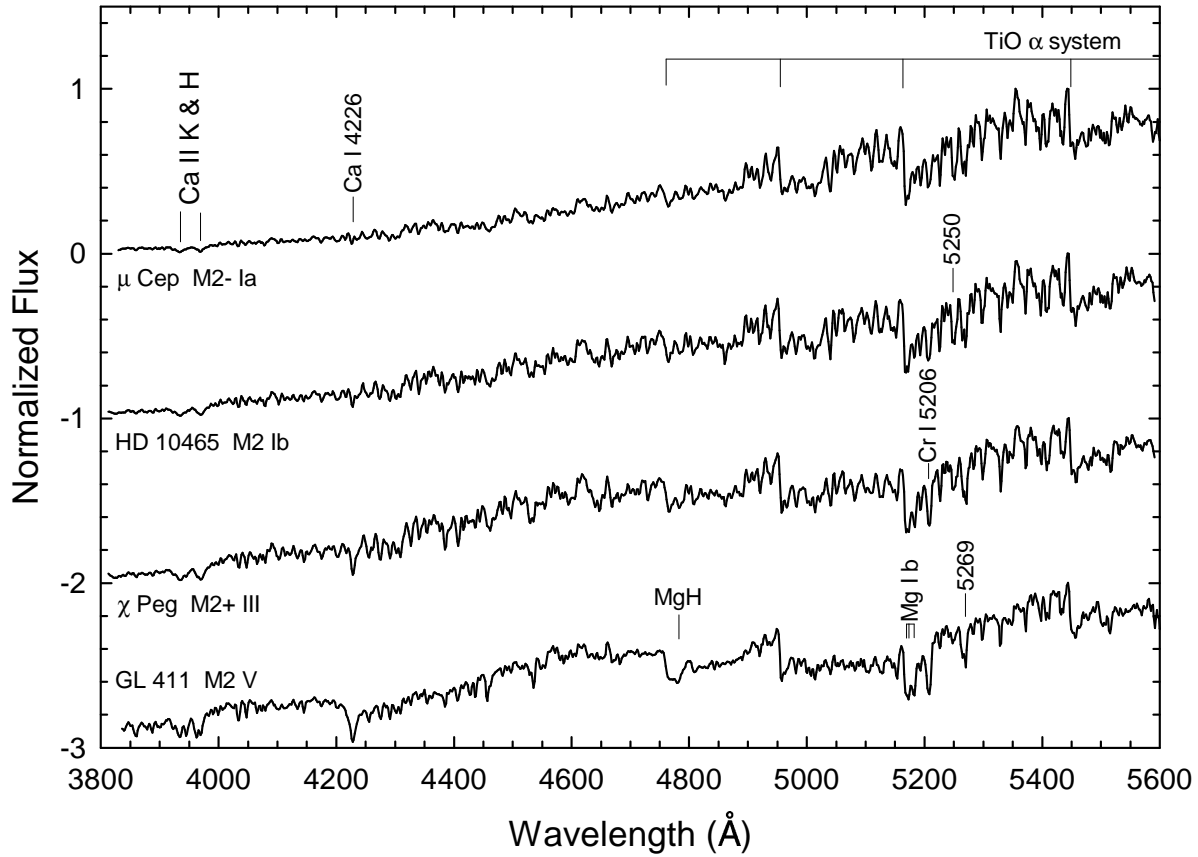
Luminosity Effects at M2

Figure 32: Luminosity Effects at M2. DSO 3.6Å resolution spectra.

The negative luminosity effect in the Ca I $\lambda 4226$ line is the most striking luminosity indicator in the M2 stars. At this resolution, the morphology of the MgH/TiO blend near 4770Å can be used as well to distinguish luminosity classes; notice that the MgH band dominates this blend in the dwarf star, producing a tooth-shaped feature. The morphology of the spectral region between 4900 and 5200Å seems to be quite sensitive to luminosity. In addition, the ratio of two blends at 5250Å and 5269Å continues to be luminosity sensitive. At higher resolutions, other features, especially in the blue-violet region, can be used.
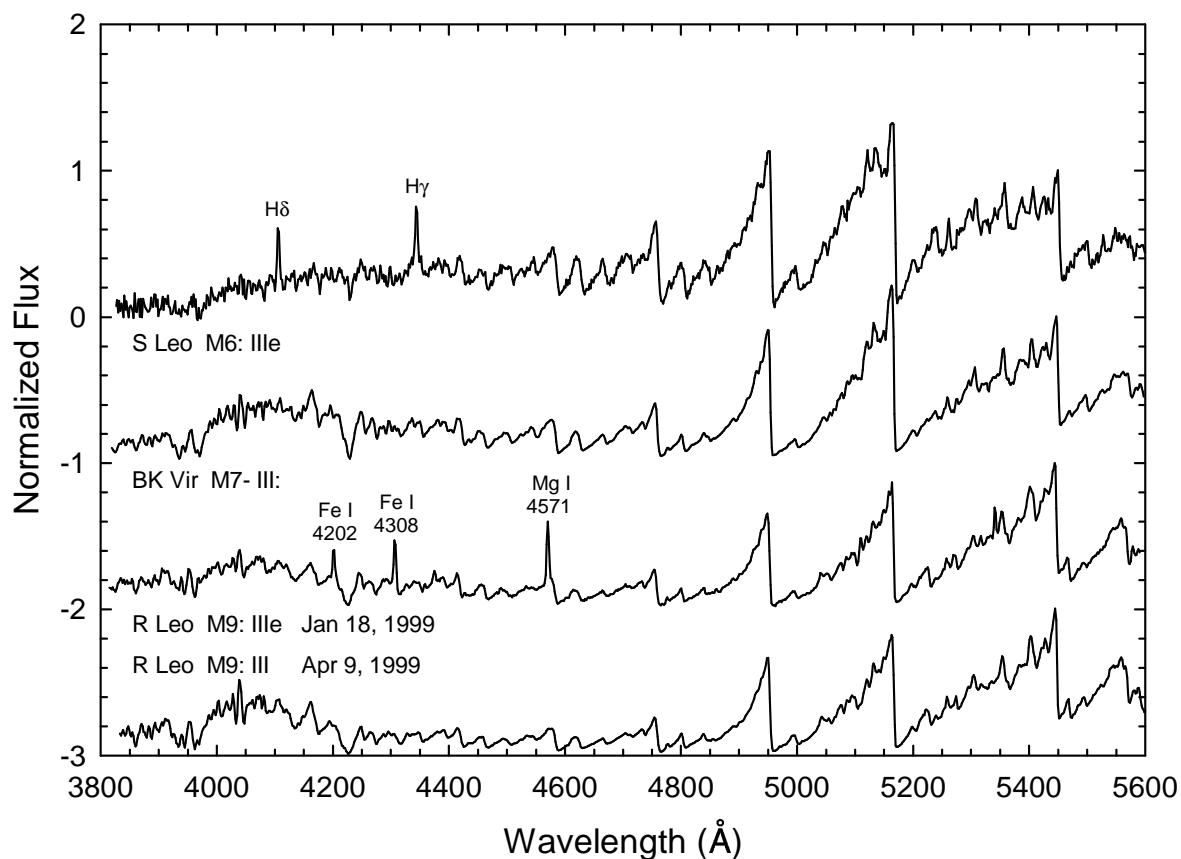
Emission Lines in Mira Variable Stars

Figure 33: Mira variable spectra at different phases. S Leo and R Leo are both long-period (Mira) variables. Note the appearance of Balmer emission lines in the spectrum of S Leo and fluorescence emission lines due to metals in R Leo. The fourth spectrum is also of R Leo, taken at a phase without obvious emission; at this phase the spectral type is approximately M9 III. DSO 3.6Å resolution spectra.

The Mira variable stars are defined as M-type stars with periods of $80 - 1000$ days and amplitudes greater than 2.5 magnitudes. The spectra of these giant pulsating stars show dramatic changes during the pulsation cycle, and even show spectral differences from cycle to cycle. Shock waves in the pulsating atmospheres of these stars produce emission lines in their spectra. The hydrogen lines are usually in emission, with the emission strength increasing toward maximum light, although the Balmer decrement is quite often unusual. Note that in S Leo (top spectrum), $H\delta$ and $H\gamma$ are quite strong, but $H\beta$ is not visible. In R Leo (third spectrum), the hydrogen lines are not strongly in emission, but emission lines of Fe I (4202, 4308) and Mg I 4571 are visible. In many stars the hydrogen-line emission strength is in antiphase with the emission lines of Fe I and Mg I.

Mira variable stars can also show a number of other interesting phenomena. Many Mira stars show a "washed-out" appearance to their spectra at the faintest phases in which the TiO bands lose contrast, and the atomic lines appear broader and shallower. This phenomenon has been referred to as "veiling", and may be due to the formation of high-level atmospheric clouds. In addition, Miras can show spectral bands due to AlO at certain phases.
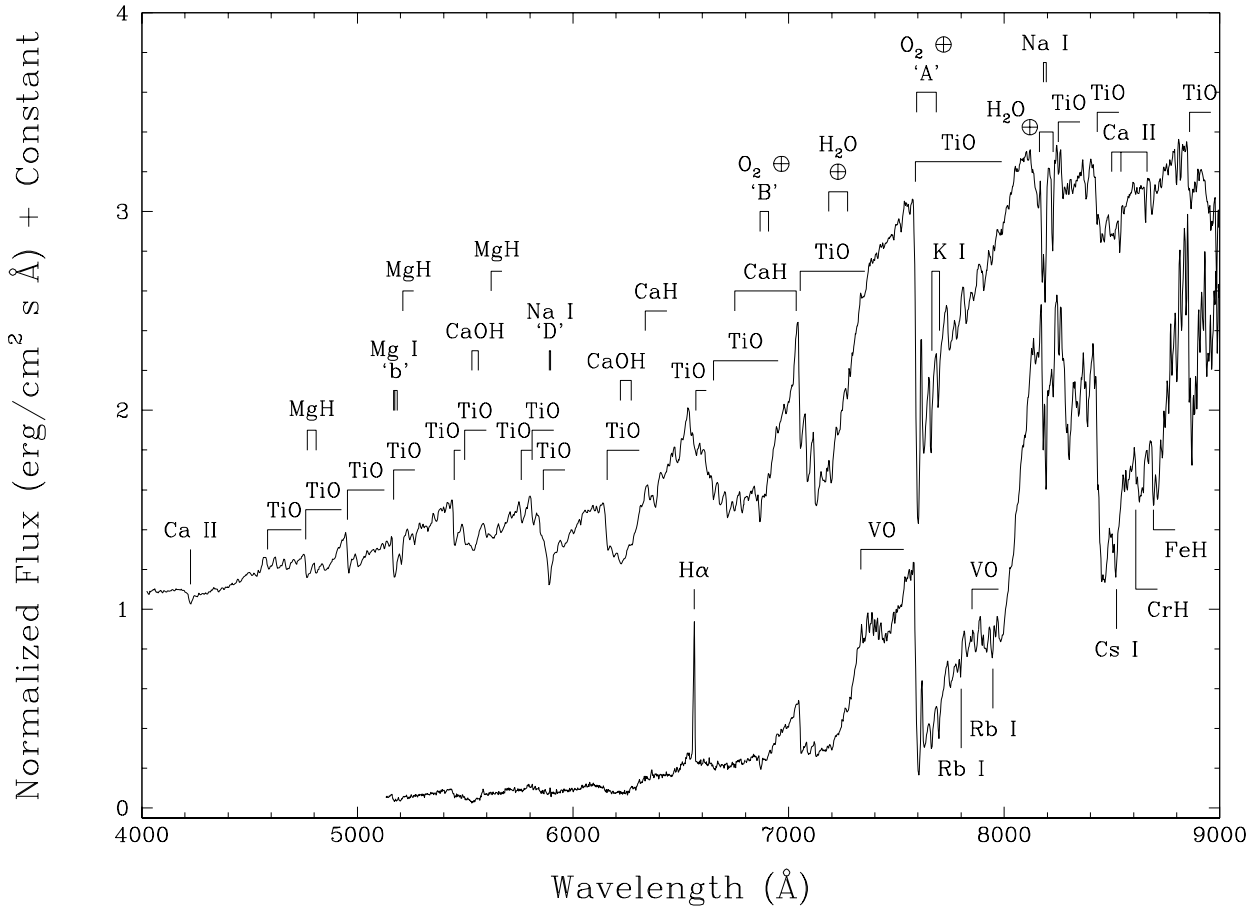
Late M-type dwarfs

Figure 34: Optical spectra of the M4.5 dwarf v And B and the M9 dwarf LHS 2065. Line and band identifications are marked on the M4.5 dwarf. Additional features appearing at cooler temperatures are marked on the spectrum of the late-M dwarf. Reproduced from *Stellar Spectral Classification*, courtesy J. Davy Kirkpatrick.

Increasingly strong TiO absorption and declining effective temperatures in the late M-type dwarfs greatly decrease the flux in the traditional spectral classification region (3800 – 5000Å), necessitating a shift to the red and near infrared to classify the cool dwarfs. At M4.5, the spectrum is dominated by absorption bands of TiO; MgH continues to contribute strong features that are luminosity sensitive (see Figure 32); in the red CaH plays a similar role. In the very cool M9 dwarf, bands of VO become prominent, as well as features due to FeH and CrH. Lines of alkaline metals, such as Rb I and Cs I are also strong.
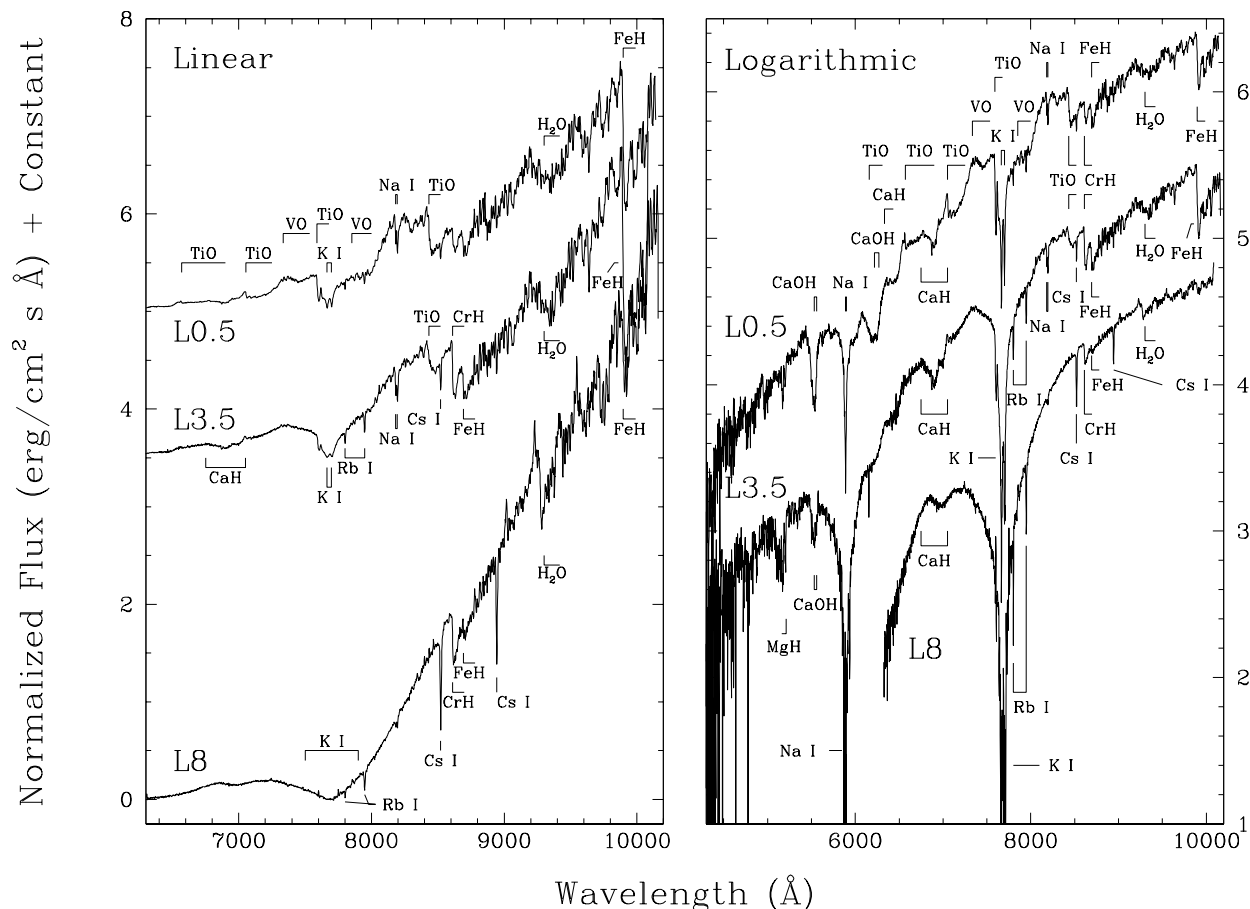
The L-type dwarfs

Figure 35: A temperature sequence for the L-type dwarfs in the red-optical. Shown are an early-, mid-, and late-L dwarf on both a linear (left) and logarithmic (right) flux scaling. Note the fading of the TiO and VO bands and the increasing importance of the metallic hydrides and lines of alkaline metals. Reproduced from *Stellar Spectral Classification*, courtesy J. Davy Kirkpatrick.

Early-L dwarfs show a melange of atomic and molecular bands in the optical, the most prominent being the neutral alkali lines (Na I, K I, Rb I, Cs I, and sometimes Li I), oxide bands TiO and VO, hydride bands CrH and FeH, and CaOH. By mid-L the resonance lines of Na I and K I have grown tremendously in strength; the hydrides MgH, CaH, CrH, and FeH have also strengthened, whereas the oxides TiO and VO have largely disappeared. By late-L, H_2O has increased in strength, the neutral alkali lines are still strong, and the hydrides are much reduced in prominence.

The M and L-dwarfs form a continuum of types describing main-sequence stars and brown dwarfs. This sequence can continue to be understood as a temperature sequence.

The disappearance of TiO and VO from the spectra of mid L dwarfs is due to formation of condensates such as perovskite ($CaTiO_3$) and their consequent removal from the atmosphere.

Which spectral type corresponds to hydrogen-burning stars and which to brown dwarfs really depends upon the age of the object. Early to mid-M dwarfs are composed exclusively of hydrogen-burning stars. Mid- to late-M dwarfs are comprised of old, low-mass stars (down to a mass of $\sim 0.085 M_\odot$ and young brown dwarfs. Early- to mid-L dwarfs are a mixture of low-mass stars that are fairly old, and brown dwarfs generally younger than about 3 Gyr. The latest L dwarfs are, however, all brown dwarfs. Because some M dwarfs are brown dwarfs and some L dwarfs are stars, it is best to refer to all these objects as "dwarfs" rather than "stars".
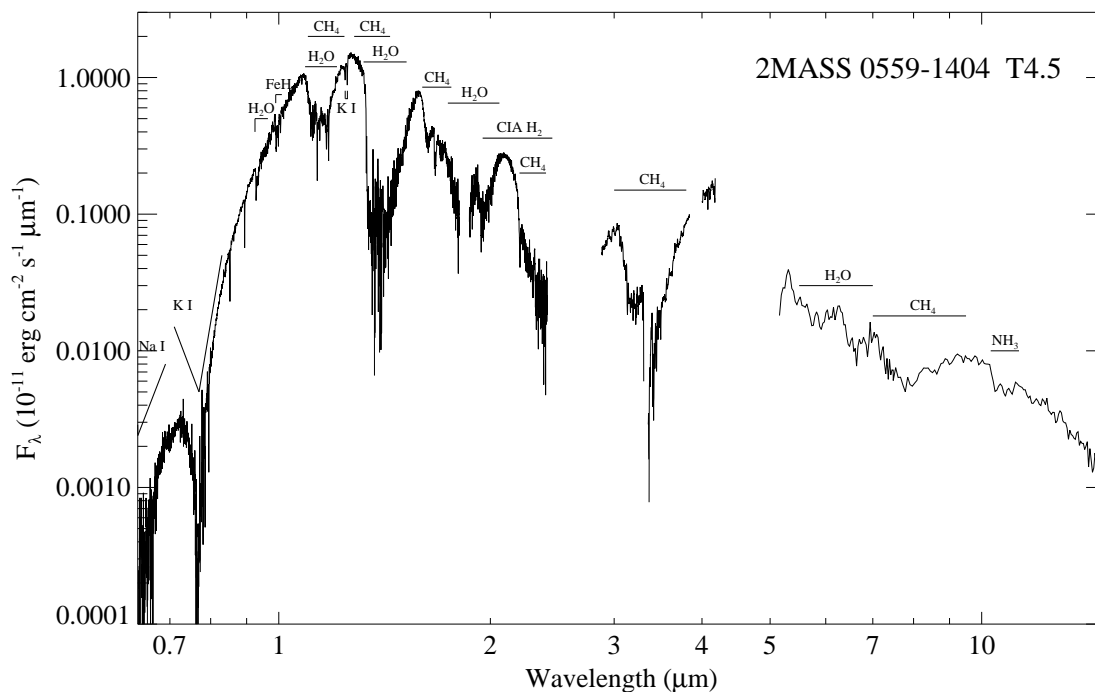
The T Dwarfs

Figure 36: The spectrum of a mid-T dwarf spanning the wavelengths $0.63 - 15\mu$m. Prominent atomic and molecular features are labeled. Reproduced from *Stellar Spectral Classification*, courtesy Adam Burgasser.

Figure 36 shows the spectrum of a typical mid-T dwarf from the red to the mid-infrared. In the red, the spectral energy distribution is shaped by the very extensive wings of the K I resonance line; in the far red and infrared, the most prominent features are due to CH_4 and H_2O. Indeed, T dwarfs are distinguished from the L dwarfs by the presence of CH_4 absorption in their near-infrared and infrared spectra. Figure 37 shows a sequence of T dwarfs, including the transition from L dwarfs to T dwarfs.

The continuous change in spectral shape along the sequence illustrated in Figure 37 is due, primarily, to increasing absorption in the CH_4 bands at 1.15, 1.35, 1.65 and 2.2 μm. There is another important CH_4 band at 3.3 μm. All T dwarfs are brown dwarfs.
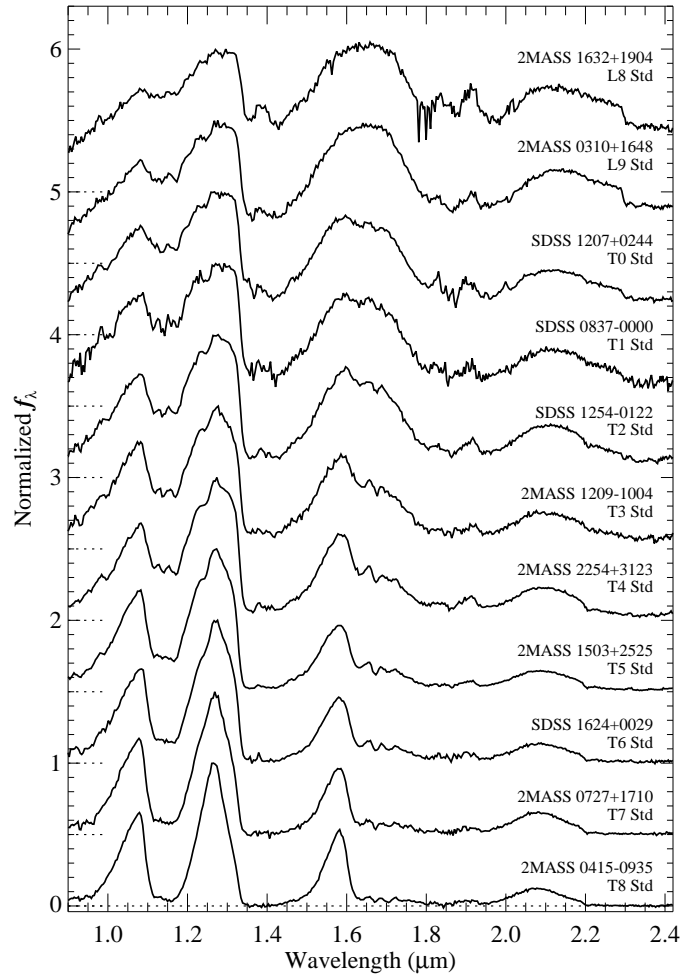
Figure 37: A spectral sequence from the late-L dwarfs through the T dwarfs in the near infrared. Feature identifications may be determined from Figure 36. Reproduced from *Stellar Spectral Classification*, courtesy Adam Burgasser.

Carbon Stars

Most known carbon stars are cool giants, although carbon dwarfs exist as well, and may even turn out to be the most common type of carbon star. Carbon stars are characterized by strong bands of carbon molecules, including bands of C_2, CN, and CH. A number of types of carbon star are recognized on the latest revision of the carbon-star classification system (Keenan, 1993; Barnbaum, Stone & Keenan, 1996), including the C-R, C-N, C-J, and C-H stars. Low-resolution spectra of the C-R and C-N carbon stars are shown in the following two figures, a higher resolution montage in the blue illustrating the C-J stars and finally a low-resolution montage for the C-H stars.
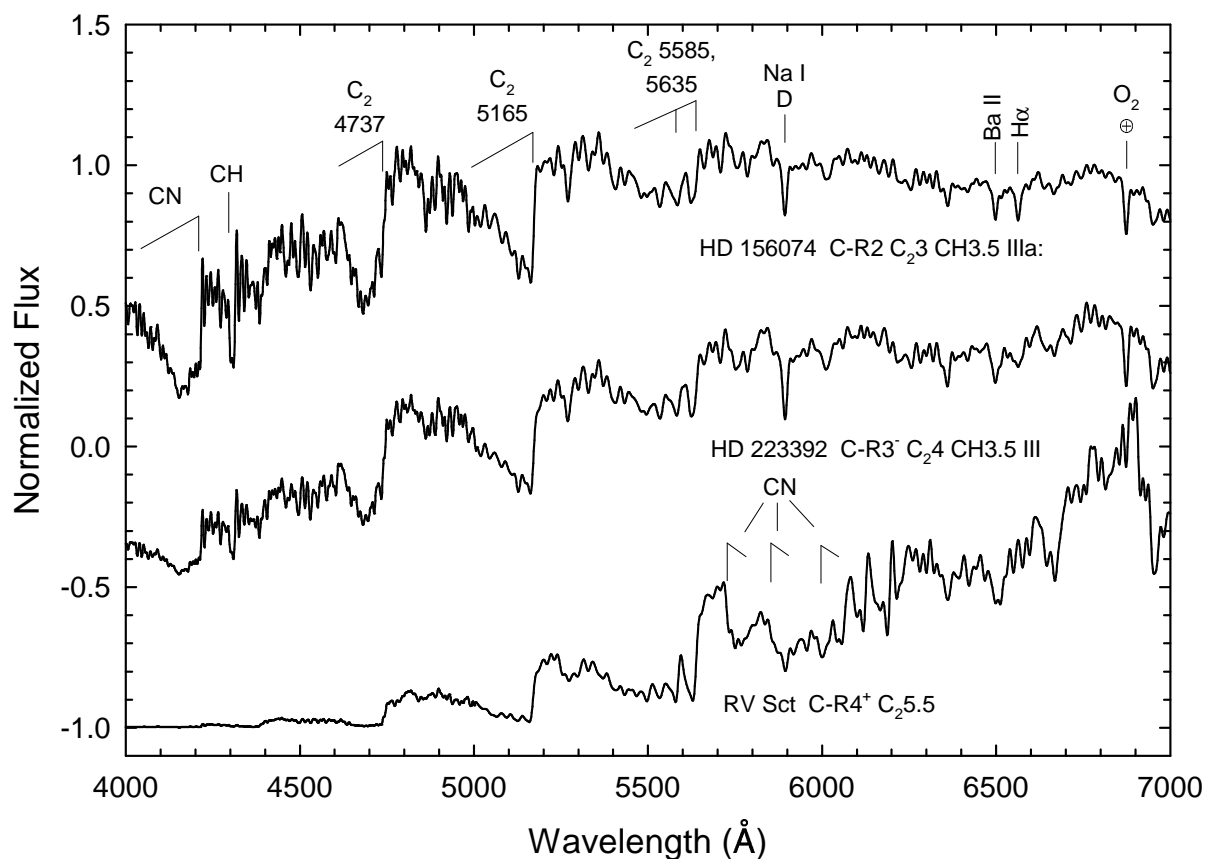

Figure 38: A low-resolution temperature sequence for the carbon R-type stars on the Keenan 1993 system. The most prominent features have been labeled, including the Swan bands of C_2. Spectra and spectral types from Barnbaum, Stone & Keenan (1996).

The C-R stars are the warmest of the carbon stars, corresponding in effective temperature to the G and K giants, and thus the early C-R stars are generally characterized by appreciable flux in the blue-violet. While the prominent bands of carbon molecules obscure a number of classification criteria used in the oxygen-rich G and K giants, a number of criteria,

including the metallicity-independent ratio of the Cr I $\lambda4254$ resonance line with neighboring subordinant Fe I lines may be used. For those stars in which the Balmer lines are visible, the Hγ/Fe I $\lambda4383$ ratio may be used. The s-process elements (such as Sr, Y, and Ba) are not usually enhanced in the C-R stars, and this is one of the major criteria distinguishing them from the C-N stars. Thus, luminosity criteria employing lines of those species may be used with caution in the C-R stars. The isotopic bands of C_2, especially those of $^{12}C^{13}C$ (which are most easily seen near the $\lambda4737$ bandhead – see Figure 40) are usually quite prominent in the C-R stars.
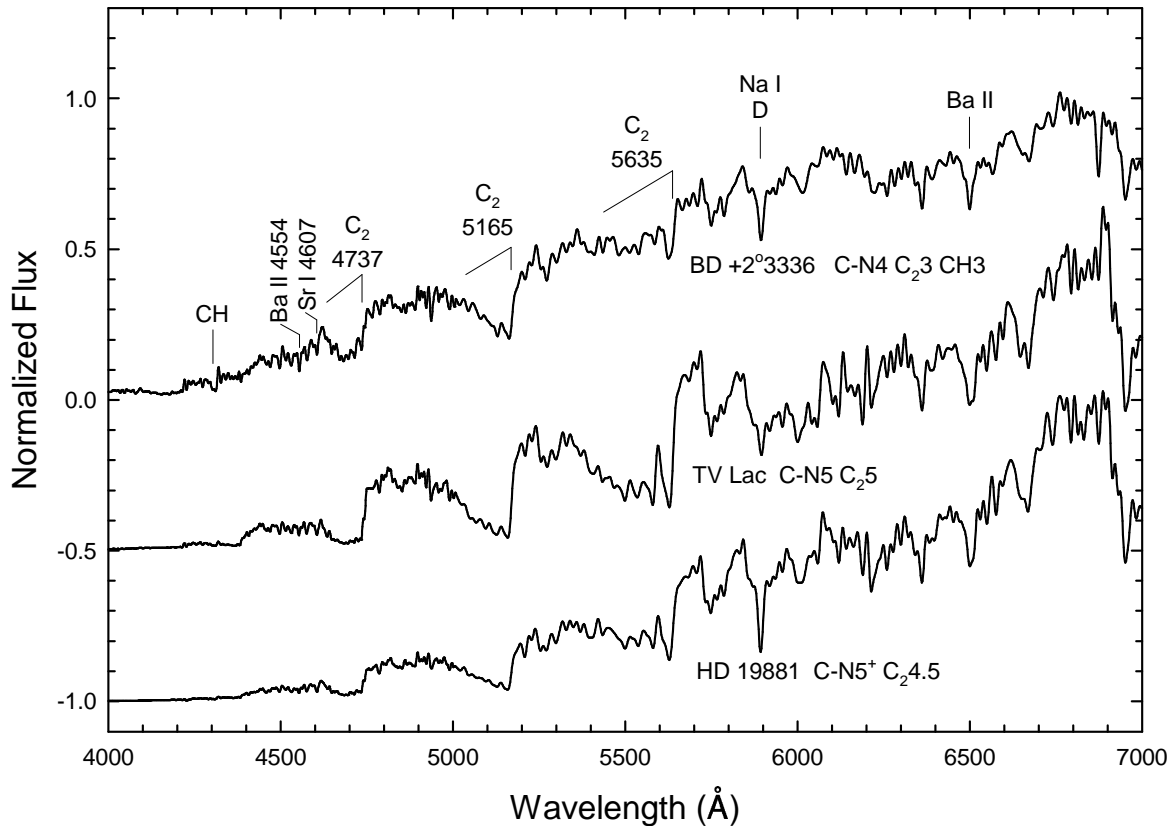

Figure 39: A low-resolution temperature sequence for the carbon N-type stars on the Keenan 1993 system. The most prominent features have been labeled, including the Swan bands of C_2. Spectra and spectral types from Barnbaum, Stone & Keenan (1996).

The C-N stars can be distinguished from the C-R stars by their extreme redness and by strong absorption in the blue, with generally little or no flux shortward of 4400Å. The C_2 isotopic bands in the C-N stars are generally weaker than in the C-R stars, but lines of s-process elements are stronger in the C-N stars. The temperature criteria mentioned above are generally unusable in the C-N stars because of the lack of violet flux. Instead, the primary temperature criterion employed is the ratio Ba II $\lambda4554$/Sr I $\lambda4607$.
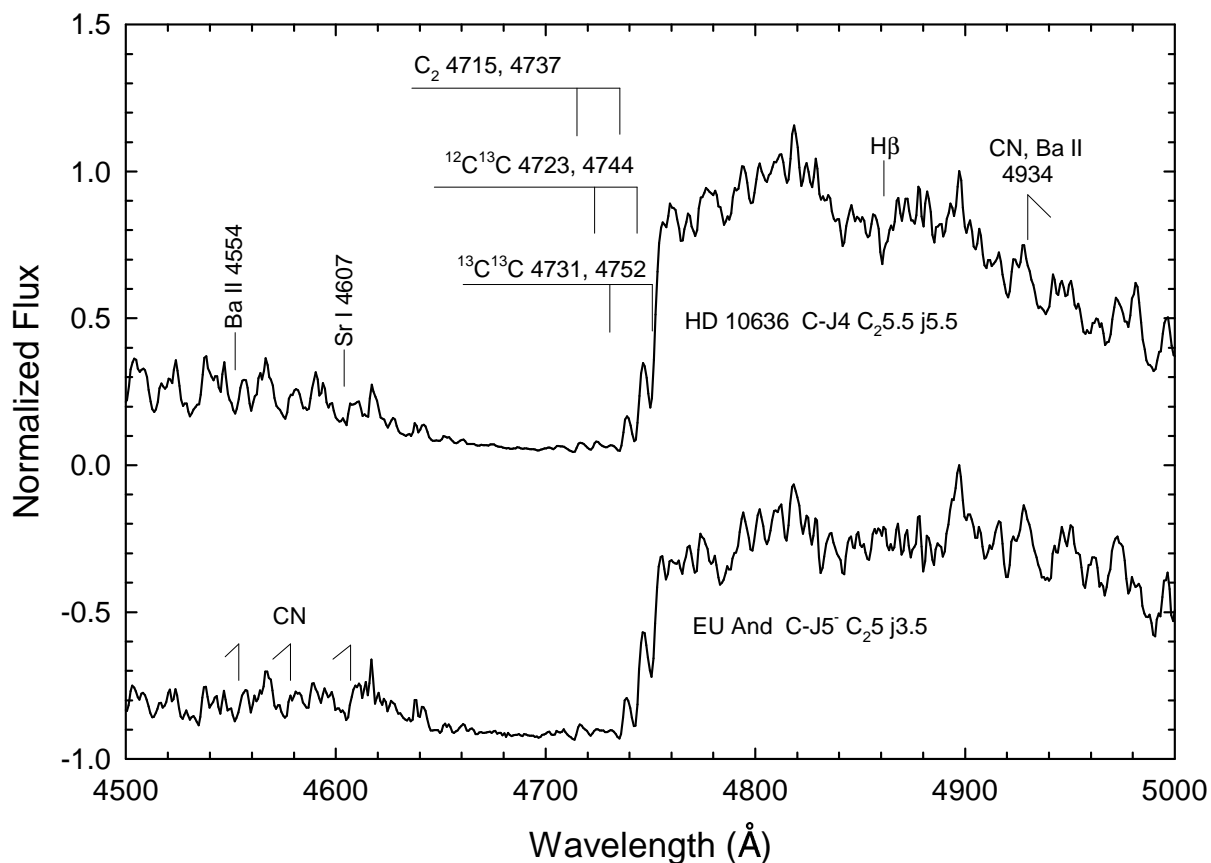
Figure 40: A high-resolution temperature sequence of C-J stars in the blue. Note the strong isotopic $^{13}C^{13}C$ bandhead at $\lambda 4752$ in both of these stars. Spectra and spectral types from Barnbaum, Stone & Keenan (1996).

The C-J stars are carbon stars that show a remarkably large abundance of the isotope ^{13}C, and thus prominent $^{12}C^{13}C$ and even $^{13}C^{13}C$ bands (see Figure 40). C-J stars generally have effective temperatures between those of the C-R and the C-N stars. The C-J stars may be further distinguished from the C-N stars by the fact that the s-process elements are not usually enhanced.

Finally, the spectra of the C-H stars are dominated by bands of CH in the blue-violet region. While the G-band (which is formed from the Q-branches of the CH A–X 0–0 and 1–1 bands located near 4300Å) is exceptionally strong in these stars, this is not unusual for early carbon stars; indeed the G-band is quite often saturated in the spectra of early carbon stars. Instead, the distinguishing spectral feature of these stars is the strength of the P-branches of these same CH bands, which are visible as a broad depression longwards of the G-band. The C-H stars overlap the C-R stars and the early C-J stars in temperature, but they differ from these classes in that they show enhancements of the s-process elements.
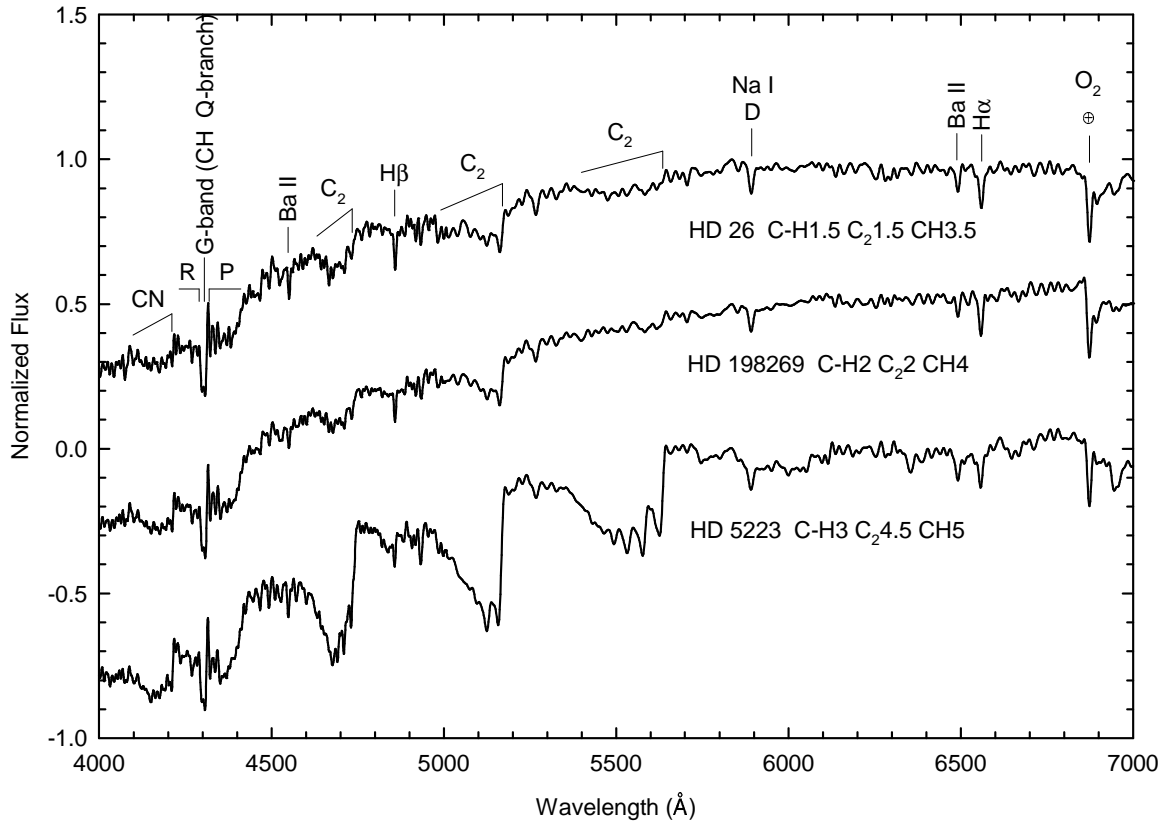
Figure 41: A low-resolution temperature sequence for the C-H stars on the Keenan 1993 system. The most prominent features have been labeled. Note the strength of the P-branch of the CH band, a distinguishing feature of these stars. Spectra and spectral types from Barnbaum, Stone & Keenan (1996).
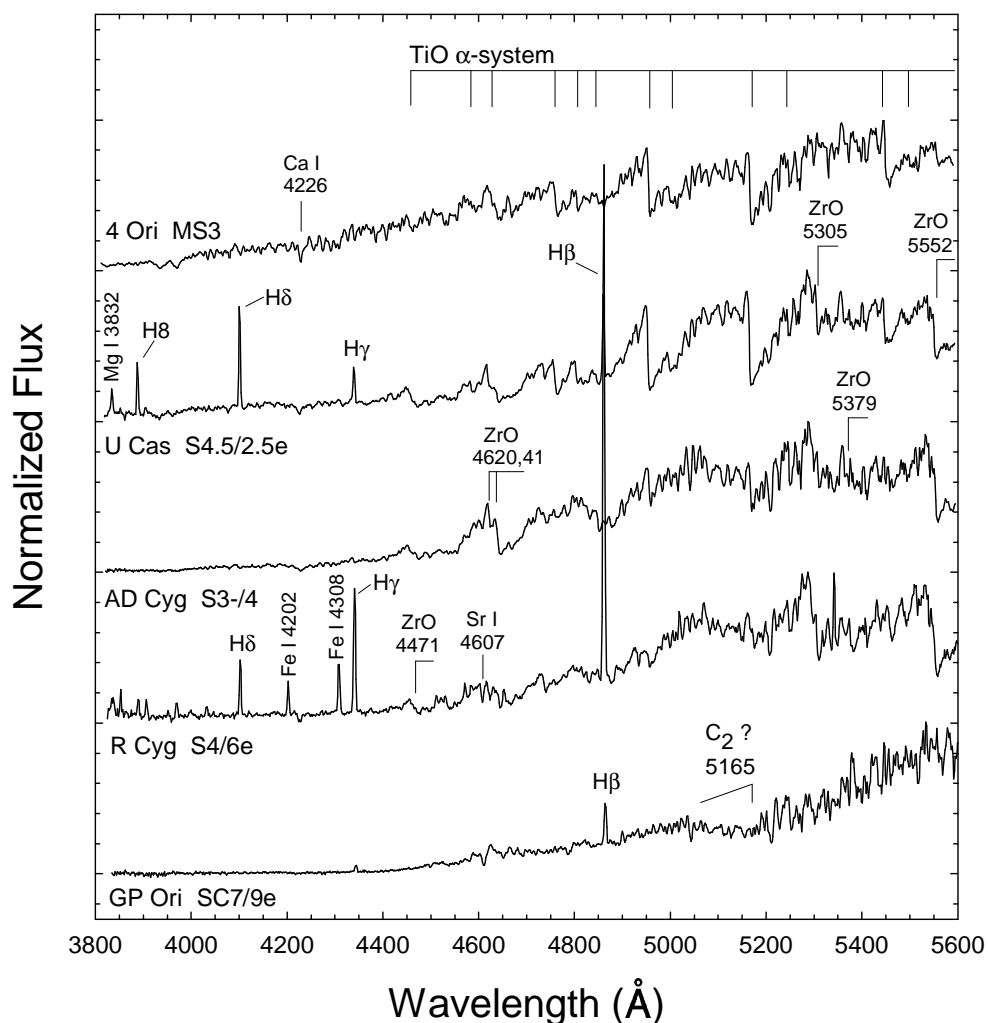
The S-type Stars

Figure 42: A sequence of S-type stars with increasing C/O index. Some of these stars are Mira variables and show emission lines at certain phases. DSO 3.6Å spectra.

If the G-, K-, and M-type giants represent the oxygen-rich temperature sequence, and the carbon stars the carbon-rich sequence, the S-type stars are those stars in which the C/O ratio is close to unity. Under such conditions, molecular equilibrium involving the CO molecule leads to the dissociation of the fragile TiO and VO molecules. The more robust molecules ZrO, YO, and LaO, involving *s*-process elements enhanced in the S-type stars, can survive until C/O is nearly unity, at which point they also dissociate. Once C/O > 1, carbon molecules appear. Thus the passage of the C/O ratio through unity, *s*-process enhancement,

and molecular equilibrium underly the M → MS → S → SC → C sequence, illustrated in the figure above. The format of the S-type spectral type takes the form

SX/n[e] ZrO TiO D YO Li

where "X" stands for the temperature type on the scale of the M-giants, "n" for the C/O index, determined on the basis of the strength of the ZrO bands relative to the TiO bands, or the presence or absence of C_2 bands, and finally, visual numerical estimates, on an arbitrary scale, of the strengths of various molecular (ZrO, TiO, YO) and atomic (Na D, Li) features may be appended to the spectral type.
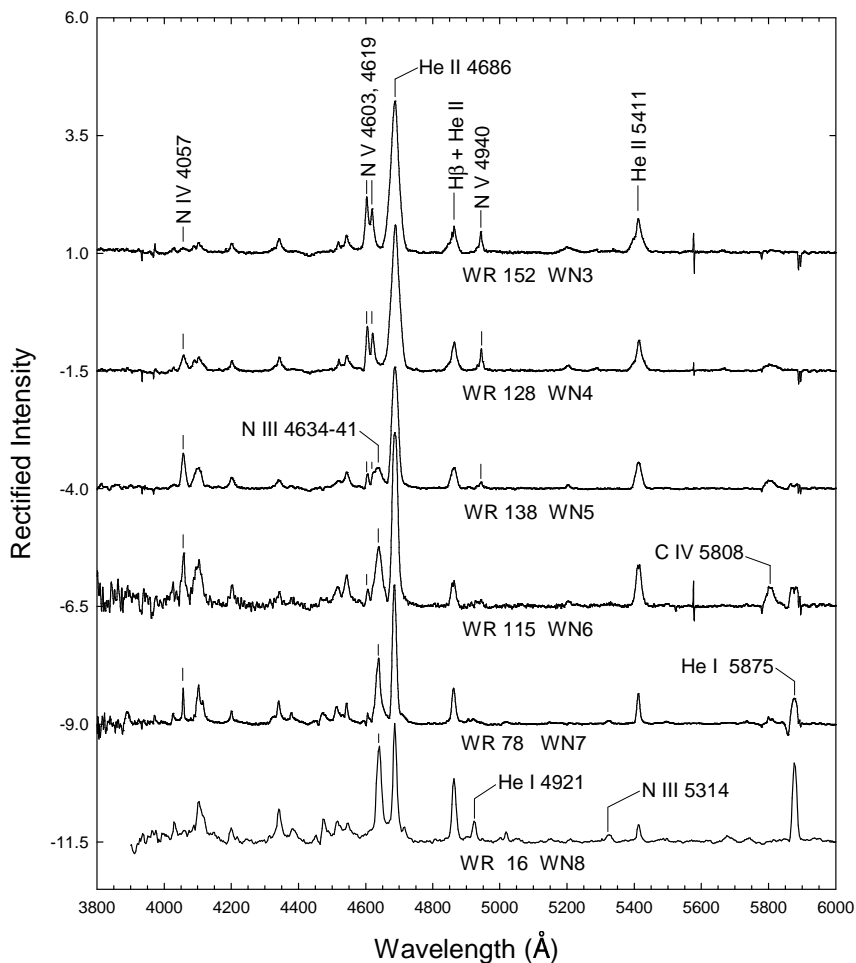
The Wolf–Rayet Stars

Figure 43: An ionization montage of the nitrogen sequence of Wolf–Rayet stars. Reproduced from *Stellar Spectral Classification*; spectra courtesy Hamann, Koesterke & Wessolowski (1995).

The Wolf–Rayet stars are luminous, hot stars whose spectra are dominated by broad, strong emission lines formed in massive stellar winds expanding outwards with velocities on the order of 1000 − 2500 km/s. Wolf–Rayet stars are among the most luminous stars in

the galaxy. Wolf–Rayet stars can be arranged into essentially two sequences, the nitrogen sequence and the carbon sequence. The nitrogen sequence (the WN stars) shows many emission lines of ionized nitrogen, whereas the carbon sequence (the WC stars) have spectra dominated by emission lines of ionized carbon.
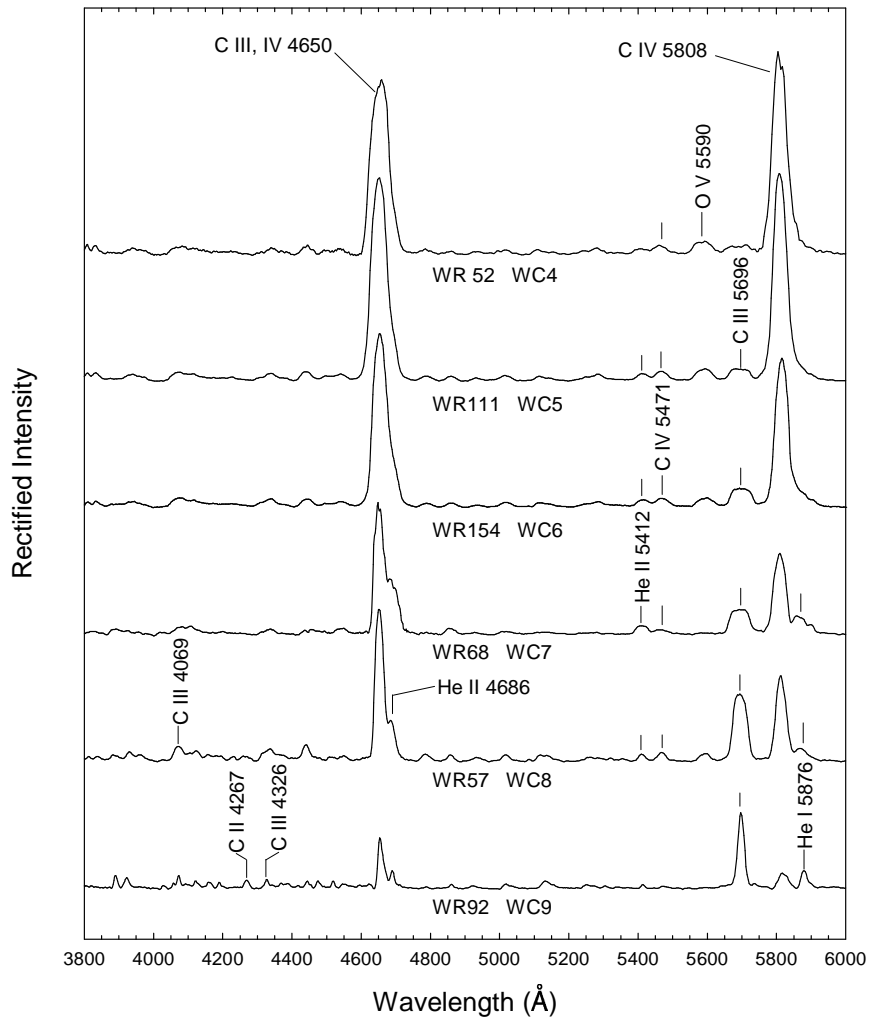

Figure 44: An ionization montage of the carbon sequence of Wolf–Rayet stars. Reproduced from *Stellar Spectral Classification*; spectra from Torres & Massey (1987).

The basic classification system for both the nitrogen and carbon Wolf–Rayet stars was

elaborated by Smith (1968), although that system has been extensively revised since then. The current classification system for the WN stars is based primarily on the He II $\lambda5411$/He I $\lambda5875$ ratio. This ratio traces out an *ionization* sequence as opposed to a *temperature* sequence, reflecting ionization conditions in the stellar wind. Secondary criteria determining the ionization class involve ratios of different ionization states of nitrogen, such as the N V $\lambda4604$/N III $\lambda4640$ ratio. WN stars are also classified on the basis of line width and hydrogen content.

The (ionization) classification of the WC stars is based on three main criteria, the C III $\lambda5696$/O V $\lambda5590$ and C III $\lambda5696$/C IV $\lambda5808$ ratios and the width of the C III,IV $\lambda4650$ blend.

There is a third sequence of Wolf–Rayet stars, the WO sequence, whose members have spectra dominated by emission lines of ionized oxygen. These rare stars probably represent the high ionization continuation of the WC stars.

References

Barnbaum, C., Stone, R.P.S. & Keenan, P.C. 1996, ApJS, 105, 419

Gray, R.O. 1989, AJ, 98, 1049

Gray, R.O. & Corbally, C.J. 1998, AJ, 116, 2530

Hamann, W.-R., Koesterke, L. & Wessolowski, U. 1995, AApS, 113, 459

Keenan, P.C. 1993, PASP, 105, 905

Keenan, P.C. & McNeil, R.C. 1976, *An Atlas of Spectra of the Cooler Stars: Types G, K, M, S and C* (Columbus: Ohio State University)

Lesh, J.R. 1968, ApJS, 16, 371

Morgan, W.W., Abt, H.A. & Tapscott, J.W. 1978, *Revised MK Spectral Atlas of Stars Earlier than the Sun* (Chicago and Tucson: Yerkes Observatory, University of Chicago, and Kitt Peak National Observatory)

Morgan, W.W., Keenan, P.C. & Kellman, E. 1943, *An Atlas of Stellar Spectra* (Chicago: University of Chicago Press)

Smith, L.F. 1968, MNRAS, 138, 109

Torres, A.V. & Massey, P. 1987, ApJS, 65, 459